Electron–Ion, Ion–Ion, and Neutral–Neutral Recombination Processes

58

Edmund J. Mansky II and M. Raymond Flannery

Contents

Abstract

This chapter collects together the formulae, expressions, and specific equations that cover various aspects, approximations, and approaches to electron–ion, ion–ion and neutral–neutral recombination processes. The primary focus is on recombination processes in the gas phase, both at thermal energies and in ultracold regimes.

Recombination processes are ubiquitous in nature. These reactions occur in a wide variety of applications and are an important formation or loss mechanism of atoms and molecules. To illustrate the types of problems where recombination is important, we enumerate six broad areas in which recombination processes occur: (a) collisional-radiative recombination processes, involving hydrogen

E. J. Mansky II (✉)
Eikonal Research Institute
Bend, OR, USA
e-mail: mansky@mindspring.com

G.W.F. Drake (Ed.), *Springer Handbook of Atomic, Molecular, and Optical Physics*, Springer Handbooks,
https://doi.org/10.1007/978-3-030-73893-8_58

and helium, which are important in understanding the cosmic microwave background in cosmology [1–3]; (b) radio recombination lines involving electrons and ions, which are central to understanding the observed spectra from interstellar clouds and planetary nebulae [4, 5]; (c) recombination processes, involving electrons and holes are important in semiconductors [6, 7]; (d) electron–ion and ion–ion recombination processes, which are important in understanding the properties of plasmas, whether they are in the upper atmosphere, the solar corona, or industrial reactors on earth [8–10]; (e) atom–molecule recombination involving oxygen, which are important mechanism for forming ozone [11]; and, finally, (f) three-body recombination processes, involving neutral bosons, which are an important loss mechanism in ultracold Rydberg atom collisions, leading to the depletion of the Bose Einstein condensate (BEC) [12–14].

Keywords

radiative recombination · mutual neutralization · dielectronic recombination · dissociative recombination · vibrational wave function

58.1 Recombination Processes

58.1.1 Electron–Ion Recombination

This proceeds via the following four processes:

(a) Radiative recombination (RR)

$$\mathrm{e}^- + \mathrm{A}^+(i) \rightarrow \mathrm{A}(n\ell) + h\nu \ . \tag{58.1}$$

(b) Three-body collisional-radiative recombination

$$\mathrm{e}^- + \mathrm{A}^+ + \mathrm{e}^- \rightarrow \mathrm{A} + \mathrm{e}^- \ , \tag{58.2a}$$

$$\mathrm{e}^- + \mathrm{A}^+ + \mathrm{M} \rightarrow \mathrm{A} + \mathrm{M} \ , \tag{58.2b}$$

where the third body can be an electron or a neutral gas.

(c) Dielectronic recombination (DLR)

$$\mathrm{e}^- + \mathrm{A}^{Z+}(i) \rightleftharpoons \left[\mathrm{A}^{Z+}(k) - \mathrm{e}^-\right]_{n\ell} \rightarrow \mathrm{A}^{(Z-1)+}_{n'\ell'}(f) + h\nu \ , \tag{58.3}$$

(d) Dissociative recombination (DR)

$$\mathrm{e}^- + \mathrm{AB}^+ \rightarrow \mathrm{A} + \mathrm{B}^* \ . \tag{58.4}$$

Electron recombination with bare ions can proceed only via (a) and (b), while (c) and (d) provide additional pathways for ions with at least one electron initially or for molecular ions AB^+. Electron radiative capture denotes the combined effect of RR and DLR.

Field-assisted:
Electron–ion recombination can also occur by application of a laser field,

$$\mathrm{e}^- + \mathrm{A}^+(i) + h\nu \rightarrow \mathrm{A}(n\ell) + h\nu' \ , \tag{58.5}$$

leading to high-order harmonic generation (HHG).

58.1.2 Positive–Ion Negative–Ion Recombination

This proceeds via the following three processes:

(e) Mutual neutralization

$$\mathrm{A}^+ + \mathrm{B}^- \rightarrow \mathrm{A} + \mathrm{B}^* \ . \tag{58.6}$$

(f) Three-body (termolecular) recombination

$$\mathrm{A}^+ + \mathrm{B}^- + \mathrm{M} \rightarrow \mathrm{AB} + \mathrm{M} \ . \tag{58.7}$$

(g) Tidal recombination

$$\mathrm{AB}^+ + \mathrm{C}^- + \mathrm{M} \rightarrow \mathrm{AC} + \mathrm{B} + \mathrm{M} \tag{58.8a}$$

$$\rightarrow \mathrm{BC} + \mathrm{A} + \mathrm{M} \ , \tag{58.8b}$$

where M is some third species (atomic, molecular, or ionic). Although (e) always occurs when no gas M is present, it is greatly enhanced by coupling to (f). The dependence of the rate $\hat{\alpha}$ on density N of background gas M is different for all three cases, (e)–(g).

Processes (a), (c), (d), and (e) are elementary processes in that microscopic detailed balance (proper balance) exists with their true inverses, i.e., with photoionization (both with and without autoionization) as in (c) and (a), associative ionization and ion-pair formation as in (d) and (e), respectively. Processes (b), (f), and (g) in general involve a complex sequence of elementary energy-changing mechanisms as collisional and radiative cascade and their overall rates are determined by an input–output continuity equation involving microscopic continuum-bound and bound–bound collisional and radiative rates.

58.1.3 Balances

Proper Balances
Proper balances are detailed microscopic balances between forward and reverse mechanisms that are direct inverses of one another, as in

(a) Maxwellian: $\mathrm{e}^-(v_1) + \mathrm{e}^-(v_2) \rightleftharpoons \mathrm{e}^-(v_1') + \mathrm{e}^-(v_2') \ ,$ (58.9)

where the kinetic energy of the particles is redistributed;

$$\text{(b)} \qquad \text{Saha: } e^- + H(n\ell) \rightleftharpoons e^- + H^+ + e^- \qquad (58.10)$$

between direct ionization from and direct recombination into a given level $n\ell$;

$$\text{(c)} \qquad \text{Boltzmann: } e^- + H(n\ell) \rightleftharpoons e^- + H(n', \ell') \qquad (58.11)$$

between excitation and deexcitation among bound levels;

$$\text{(d)} \qquad \text{Planck: } e^- + H^+ \rightleftharpoons H(n\ell) + h\nu \ , \qquad (58.12)$$

which involves interaction between radiation and atoms in photoionization/recombination to a given level $n\ell$.

Improper Balances

Improper balances maintain constant densities via production and destruction mechanisms that are not pure inverses of each other. They are associated with flux activity on a macroscopic level as in the transport of particles into the system for recombination and net production and transport of particles (i.e. e^-, A^+) for ionization. Improper balances can then exist between dissimilar elementary production–depletion processes as in (a) coronal balance between electron-excitation into and radiative decay out of level n. (b) Radiative balance between radiative capture into and radiative cascade out of level n. (c) Excitation saturation balance between upward collisional excitations $n-1 \rightarrow n \rightarrow n+1$ between adjacent levels. (d) Deexcitation saturation balance between downward collisional de-excitations $n+1 \rightarrow n \rightarrow n-1$ into and out of level n.

58.1.4 Neutral–Neutral Recombination

Neutral–neutral reactions, leading to recombination or dissociation, generally proceed via resonances involving transitions among molecular electronic states. At thermal energies, these reactions are studied via transition state theory, reaction rate theory, and a wide range of semiclassical techniques. See Chap. 37 of this Handbook and [15–19] for a general introduction to this vast literature in chemical physics and chemistry.

Distinguishable Particles [3]

When one or more reactants in the process are distinguishable, the thermal reactions proceed via two broad pathways, *direct* and *indirect*:

Direct pathway

$$A + B + C \xrightarrow{k_{\text{direct}}} AB + C \ , \qquad (58.13)$$

where k_{direct} is the reaction rate (cm^3/s) for the formation of molecule AB and reactant C.

Indirect pathways

$$A + B + C \begin{cases} \xrightarrow{k^{ET}_{\text{indirect}}} (A\cdots B) + C \rightarrow AB + C \\ \xrightarrow{k^{Ex}_{\text{indirect}}} (A\cdots C) + B \rightarrow AB + C \end{cases} , \qquad (58.14)$$

where $(A\cdots B)$ indicates an intermediate collision complex formed between atoms A and B, and k^{ET}_{indirect}, k^{Ex}_{indirect} are the reaction rates (cm^3/sec) for the transfer and exchange reactions in Eq. (58.14) (upper/lower), respectively. Prediction of rates k, in both the direct and indirect pathways, depends upon detailed knowledge of the molecular potential energy surfaces, curve-crossings, and tunneling probabilities for specific reactants.

LTE effective rate equation

For systems in local thermodynamic equilibrium (LTE), the effective rate equations are

$$\frac{1}{[C]}\frac{d}{dt}[AB] = k_r[A][B] - k_d[AB] \ , \qquad (58.15)$$

where the square brackets indicate the number density of the enclosed species, and k_r denotes the rate constant for three-body recombination, while k_d the rate constant for collision-induced dissociation

$$k_r = \sum_{b,u} k_{u\rightarrow b} \frac{[AB(u)]}{[A][B]} \ , \qquad (58.16a)$$

$$k_d = \sum_{b,u} k_{b\rightarrow u} \frac{[AB(b)]}{[AB]} \ , \qquad (58.16b)$$

with b and u representing bound and unbound states of the indicated collision complex, respectively. The state-to-state rate coefficients are defined by

$$k_{i\rightarrow j} = \left(\frac{8k_BT}{\pi\mu}\right)^{1/2} (k_BT)^{-2} \int_0^\infty \sigma_{i\rightarrow j}(E_T) \times \exp(-E_T/k_BT) E_T \, dE_T \ , \qquad (58.17)$$

where μ is the reduced mass, $E_T = E - E_i$ is the translational energy of the i-th state of the atom, and σ is the cross section for the indicated transition $i \rightarrow j$.

NLTE effective rate equations

For systems not in local thermodynamic equilibrium (NLTE) the effective rate equations are

$$6\frac{d}{dt}[AB(b)] = [C]\sum_u (k_{u\rightarrow b}[AB(u)] - k_{b\rightarrow u}[AB(b)]) + [C]\sum_{b'} \left(k_{b'\rightarrow b}\left[AB(b')\right] - k_{b\rightarrow b'}[AB(b)]\right) \ , \qquad (58.18a)$$

$$\frac{d}{dt}[\mathrm{AB}(u)] = [\mathrm{C}]\sum_b (k_{b\to u}[\mathrm{AB}(b)] - k_{u\to b}[\mathrm{AB}(u)]) + [\mathrm{C}]\sum_{u'}\left(k_{u'\to u}\left[\mathrm{AB}(u')\right] - k_{u\to u'}[\mathrm{AB}(u)]\right) + k_{f\to u}^{\mathrm{elastic}}[\mathrm{A}][\mathrm{B}] - \frac{[\mathrm{AB}(u)]}{\tau_u} , \quad (58.18b)$$

where τ_u is the lifetime of the unbound state u, and $k_{f\to u}^{\mathrm{elastic}}$ is the elastic two-body rate constant.

Identical Particles

At thermal energies, reactions involving identical particles proceed as detailed above. In ultracold regimes, collisions involving identical bosons proceed via Fano–Feshbach or Föster resonances [20–22]. These resonances can be exploited by varying the applied magnetic or electric fields used in traps to create and control Bose–Einstein condensates (BEC).

At thermal and higher energies, the rate-limiting step [23] is generally either collisional or radiative capture into high-lying Rydberg states ($n \gg 1$), followed by radiative decay into lower lying states via n and n, ℓ mixing collisions. In contrast, at ultracold regimes, the rate-limiting step is collisional ℓ mixing, wherein rapid collisional capture into very high-lying Rydberg states ($n > 200$) is followed by slow collisional-radiative decay. The result is a cloud of Rydberg atoms that has condensed into a long-lived macroscopic BEC, which can be controlled via the applied fields used in the trap.

For three identical particles, this proceeds as

$$\mathrm{A} + \mathrm{A} + \mathrm{A} \to \mathrm{A}_2 + \mathrm{A}(E_f) . \quad (58.19)$$

Time-dependent equation

$$\frac{dn_\mathrm{A}}{dt} = \begin{cases} -3\alpha n_\mathrm{A}^3 & \text{before onset of BEC} \\ -\frac{1}{2}\alpha n_\mathrm{A}^3 & \text{at BEC} \end{cases} , \quad (58.20)$$

where α is the recombination rate coefficient (number of dimers $\mathrm{cm}^{-3}\,\mathrm{s}^{-1}$), and n_A is the number density of atoms A. At the onset of BEC in ultracold traps, the recombination rate is reduced by the factor $1/3!$ because of the symmetry of the macroscopic quantum state the atoms A are then in. See Sect. 58.4 for explicit closed-form expressions for α.

Heteronuclear Mixtures

For heteronuclear mixtures of particles, this proceeds as

$$\mathrm{A} + \mathrm{B} + \mathrm{B} \longrightarrow \mathrm{AB} + \mathrm{B}(E_f) , \quad (58.21)$$

for distinct atoms A and B.

At thermal energies this is analyzed as above using either LTE or NLTE formulations involving the relevant molecular potential surfaces. At ultracold regimes [24] the mixtures are composed of heavy and light bosons, or bosons and fermions, or of a boson together with heavy and light fermions, and are analyzed using zero-range methods. See Table 1 of [25] for details on the various cases where the Efimov effect occurs in such systems and Sect. 58.4 for explicit expressions for α. For details on the Efimov effect, see Sects. 58.4 and 60.6 in this Handbook and [25, 26].

Time-dependent equation

$$\frac{dn_\mathrm{A}}{dt} = -\alpha n_\mathrm{A}\, n_\mathrm{B}^2 . \quad (58.22)$$

58.1.5 N-Body Recombination [27]

This proceeds, for four identical particles, as

$$\mathrm{A} + \mathrm{A} + \mathrm{A} + \mathrm{A} \longrightarrow \begin{cases} \mathrm{A}_3 + \mathrm{A}(E_f) & \text{trimer + atom} , \\ \mathrm{A}_2 + \mathrm{A}_2 & \text{dimer + dimer} , \\ \mathrm{A}_4 & \text{tetramer} , \end{cases} \quad (58.23)$$

and has been observed [28] in an ultracold sample of Cs atoms at 30 nK. See Fig. 58.1 for an illustration of the allowed regimes for the various reactant branches in (58.23) as a function of energy and inverse scattering length.

The general problem of N-body recombination is challenging both experimentally and theoretically. Samples involving alkali atoms at ultracold temperatures currently provide the best conditions for observing N-body recombination. At present, the hyperspherical method of solving the N-body Schrödinger equation has been used most extensively on the problem. See Sect. 58.5 for closed-form expressions for N-body recombination rates α.

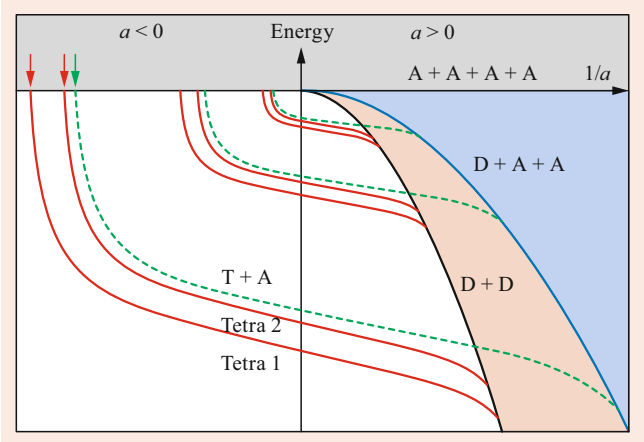

Fig. 58.1 Illustration of allowed regions for 4 bosons (A+A+A+A), Dimers + 2 bosons (D+A+A), 2 Dimers (D+D) and Trimers + bosons (T+A). See [28] for details

58.2 Collisional-Radiative Recombination

Radiative recombination
Process Eq. (58.1) involves a free-bound electronic transition with radiation spread over the recombination continuum. It is the inverse of photoionization without autoionization and favors high-energy gaps with transitions to low $n \approx 1, 2, 3$ and low angular momentum states $\ell \approx 0, 1, 2$ at higher electron energies.

Three-body electron–ion recombination
Processes Eq. (58.2a,b) favor free-bound collisional transitions to high levels n, within a few $k_B T$ of the ionization limit of A(n) and collisional transitions across small energy gaps. Recombination becomes stabilized by collisional-radiative cascade through the lower-bound levels of A. Collisions of the $e^- - A^+$ pair with third bodies become more important for higher levels of n, and radiative emission is important down to and among the lower levels of n. In optically thin plasmas this radiation is lost, while in optically thick plasmas it may be reabsorbed. At low electron densities, radiative recombination dominates with predominant transitions taking place to the ground level. For process Eq. (58.2a) at high electron densities, three-body collisions into high Rydberg levels dominate, followed by cascade, which is collision dominated at low electron temperatures T_e and radiation dominated at high T_e. For process Eq. (58.2b) at low gas densities N, the recombination is collisionally radiatively controlled while, at high N, it eventually becomes controlled by the rate of diffusional drift Eq. (58.73) through the gas M.

Collisional-radiative recombination [29]
Here, the cascade collisions and radiation are coupled via the continuity equation. The population n_i of an individual excited level i of energy E_i is determined by the rate equations

$$\frac{dn_i}{dt} = \frac{\partial n_i}{\partial t} + \nabla \cdot (n_i \boldsymbol{v}_i) \tag{58.24}$$

$$= \sum_{i \neq f} \left[n_f \nu_{fi} - n_i \nu_{if} \right] = P_i - n_i D_i \ , \tag{58.25}$$

which involve temporal and spatial relaxation in Eq. (58.24) and collisional-radiative production rates P_i and destruction frequencies D_i of the elementary processes included in Eq. (58.25). The total collisional and radiative transition frequency between levels i and f is ν_{if} and the f-sum is taken over all discrete and continuous (c) states of the recombining species. The transition frequency ν_{if} includes all contributing elementary processes that directly link states i and f, e.g., collisional excitation and deexcitation, ionization ($i \rightarrow c$) and recombination ($c \rightarrow i$) by electrons and heavy particles, radiative recombination ($c \rightarrow i$), radiative decay ($i \rightarrow f$), possibly radiative absorption for optically thick plasmas, autoionization, and dielectronic recombination.

Production rates and processes
The production rate for a level i is

$$P_i = \sum_{f \neq i} n_e n_f K^c_{fi} + n_e^2 N^+ k^R_{ci} + \sum_{f > i} n_f \left(A_{fi} + B_{fi} \rho_\nu \right) + n_e N^+ \left(\hat{\alpha}^{RR}_i + \beta_i \rho_\nu \right) \ , \tag{58.26}$$

where the terms in the above order represent (1) collisional excitation and deexcitation by e^-–A(f) collisions, (2) three-body e^-–A^+ collisional recombination into level i, (3) spontaneous and stimulated radiative cascade, and (4) spontaneous and stimulated radiative recombination.

Destruction rates and processes
The destruction rate for a level i is

$$n_i D_i = n_e n_i \sum_{f \neq i} K^c_{if} + n_e n_i S_i + n_i \sum_{f < i} \left(A_{if} + B_{if} \rho_\nu \right) + n_i \sum_{f > i} B_{if} \rho_\nu + n_i B_{ic} \rho_\nu \ , \tag{58.27}$$

where the terms in the above order represent (1) collisional destruction, (2) collisional ionization, (3) spontaneous and stimulated emission, (4) photoexcitation, and (5) photoionization.

58.2.1 Saha and Boltzmann Distributions

Collisions of A(n) with third bodies such as e^- and M are more rapid than radiative decay above a certain excited level n^*. Since each collision process is accompanied by its exact inverse the principle of detailed balance determines the population of levels $i > n^*$.

Saha Distribution
This connects equilibrium densities $\tilde{n}_i$, $\tilde{n}_e$, and $\tilde{N}^+$ of bound levels i, of free electrons at temperature T_e, and of ions by

$$\frac{\tilde{n}_i}{\tilde{n}_e \tilde{N}^+} = \left(\frac{g(i)}{g_e g^+_A} \right) \frac{h^3}{(2\pi m_e k T_e)^{3/2}} \exp(I_i / k_B T_e) \ , \tag{58.28}$$

where the electronic statistical weights of the free electron, the ion of charge $Z+1$, and the recombined $e^- - A^+$ species of net charge Z and ionization potential I_i are $g_e = 2$, g^+_A, and $g(i)$, respectively. Since $n_i \leq \tilde{n}_i$ for all i, then the Saha–Boltzmann distributions imply that $n_1 \gg n_i$ and $n_e \gg n_i$ for $i \neq 1, 2$, where $i = 1$ is the ground state.

Boltzmann Distribution

This connects the equilibrium populations of bound levels i of energy E_i by

$$\tilde{n}_i/\tilde{n}_j = [g(i)/g(j)]\exp\left[-(E_i - E_j)/k_B T_e\right] . \quad (58.29)$$

58.2.2 Quasi-Steady State Distributions

The reciprocal lifetime of level i is the sum of radiative and collisional components, and this lifetime is, therefore, shorter than the pure radiative lifetime $\tau_R \approx 10^{-7} Z^{-4}$ s. The lifetime τ_1 for the ground level is collisionally controlled and depends on n_e, and, generally, is within the range of 10^2 and 10^4 s for most laboratory plasmas and the solar atmosphere. The excited level lifetimes τ_i are then much shorter than τ_1. The (spatial) diffusion or plasma decay (recombination) time is then much longer than τ_i, and the total number of recombined species is much smaller than the ground-state population n_1. The recombination proceeds on a timescale much longer than the time for population/destruction of the excited levels. The condition for quasi-steady state, or QSS-condition, $dn_i/dt = 0$ for the bound levels $i \neq 1$, therefore, holds. The QSS distributions n_i, therefore, satisfy $P_i = n_i D_i$.

58.2.3 Ionization and Recombination Coefficients

Under QSS, the continuity Eq. (58.25) then reduces to a finite set of simultaneous equations $P_i = n_i D_i$. This gives a matrix equation that is solved numerically for $n_i\,(i \neq 1) \leq \tilde{n}_i$ in terms of n_1 and n_e. The net ground-state population frequency per unit volume ($\mathrm{cm^{-3}\,s^{-1}}$) can then be expressed as

$$\frac{dn_1}{dt} = n_e N^+ \hat{\alpha}_{CR} - n_e n_1 S_{CR} , \quad (58.30)$$

where $\hat{\alpha}_{CR}$ and S_{CR}, respectively, are the overall rate coefficients for recombination and ionization via the collisional-radiative sequence. The determined $\hat{\alpha}_{CR}$ equals the direct ($c \to 1$) recombination to the ground level supplemented by the net collisional-radiative cascade from that portion of bound-state population that originated from the continuum. The determined S_{CR} equals direct depletion (excitation and ionization) of the ground state reduced by the deexcitation collisional radiative cascade from that portion of the bound levels accessed originally from the ground level. At low n_e, $\hat{\alpha}_{CR}$ and S_{CR} reduce, respectively, to the radiative recombination coefficient summed over all levels and to the collisional ionization coefficient for the ground level.

C, $\mathcal{E}$, and S Blocks of Energy Levels

For the recombination processes in Eqs. (58.2a), (58.2b), and (58.7), which involve a sequence of elementary reactions, the $e^- - A^+$ or $A^+ - B^-$ continuum levels and the ground $A(n = 1)$ or the lowest vibrational levels of AB are, therefore, treated as two large particle reservoirs of reactants and products. These two reservoirs act as reactant and sink blocks C and S, which are, respectively, drained and filled at the same rate via a conduit of highly excited levels, which comprise an intermediate block of levels $\mathcal{E}$. This C draining and S filling proceeds, via block $\mathcal{E}$, on a timescale large compared with the short time for a small amount from the reservoirs to be redistributed within block $\mathcal{E}$. This forms the basis of QSS.

58.2.4 Working Rate Formulae

For electron–atomic–ion collisional-radiative recombination Eq. (58.2a), detailed QSS calculations can be fitted by the rate [30]

$$\hat{\alpha}_{CR} = \left(3.8\times10^{-9} T_e^{-4.5} n_e + 1.55\times10^{-10} T_e^{-0.63} + 6\times10^{-9} T_e^{-2.18} n_e^{0.37}\right) \mathrm{cm^3\,s^{-1}} , \quad (58.31)$$

which agrees with experiment for a Lyman α optically thick plasma with n_e and T_e in the range $10^9\,\mathrm{cm^{-3}} \leq n_e \leq 10^{13}\,\mathrm{cm^{-3}}$ and $2.5\,\mathrm{K} \leq T_e \leq 4000\,\mathrm{K}$. The first term is the pure collisional rate Eq. (58.61), the second term is the radiative cascade contribution, and the third term arises from collisional-radiative coupling.

For $\left(e^- - He_2^+\right)$, recombination in a high-pressure (5–100 Torr) helium afterglow, the rate for Eq. (58.2b) is [31]

$$\hat{\alpha}_{CR} = \left[(4\pm0.5)\times10^{-20} n_e\right](T_e/293)^{-(4\pm0.5)} + \left[(5\pm1)\times10^{-27} n(\mathrm{He}) + (2.5\pm2.5)\times10^{-10}\right] \times (T_e/293)^{-(1\pm1)}\mathrm{cm^3/s} . \quad (58.32)$$

The first two terms are in accord with the purely collisional rates Eqs. (58.61) and (58.64b), respectively.

58.2.5 Computer Codes

A large number of computer codes for solving the collisional-radiative equations in astrophysical plasmas and fusion plasmas are available. See Table 58.1 for details.

58.3 Macroscopic Methods

58.3.1 Resonant Capture-Stabilization Model: Dissociative and Dielectronic Recombination

The electron is captured dielectronically, Eq. (58.53), into an energy-resonant long-lived intermediate collision complex of

Table 58.1 Recombination computer codes

Name	Description	Reference/Link
ACQD	Radiative recombination of hydrogenic ions	CPC 1 (1969) 31
AAID	COLLRAD	CPC 12 (1976) 205
ADNT	CRModel	CPC 135 (2001) 135
AATR	COLRAD	CPC 44 (1987) 157
AEMA	RATIP	CPC 183 (2012) 1525
ABUV	TRIP 1	CPC 16 (1978) 129
RICO	Machine-learning recombination code for BBN	ApJSS 181 (2009) 627
RECFAST	BBN code	AA 475 (2007) 109
HYREC	Primordial hydrogen and helium recombination code	Phys. Rev. D 83 (2011) 043513
LASER	Los Alamos suite of relativistic atomic physics codes	[61] & http://aphysics2.lanl.gov/tempweb

superexcited states d, which can autoionize or be stabilized irreversibly into the final product channel f either by molecular fragmentation

$$\mathrm{e}^- + \mathrm{AB}^+(i) \underset{\nu_a}{\overset{k_\mathrm{c}}{\rightleftharpoons}} \mathrm{AB}^{**} \overset{\nu_\mathrm{s}}{\to} \mathrm{A} + \mathrm{B}^* \,, \tag{58.33}$$

as in direct dissociative recombination (DR), or by emission of radiation as in dielectronic recombination (DLR)

$$\mathrm{e}^- + \mathrm{A}^{Z+}(i) \underset{\nu_a}{\overset{k_\mathrm{c}}{\rightleftharpoons}} \left[\mathrm{A}^{Z+}(k) - \mathrm{e}^-\right]_{n\ell} \overset{\nu_\mathrm{s}}{\to} \mathrm{A}^{(Z-1)+}_{n'\ell'}(f) + h\nu \,. \tag{58.34}$$

Production Rate of Superexcited States *d*

$$\frac{\mathrm{d}n_d^*}{\mathrm{d}t} = n_\mathrm{e} N^+ k_\mathrm{c}(d) - n_d^*[\nu_\mathrm{A}(d) + \nu_\mathrm{S}(d)] \,; \tag{58.35}$$

$$\nu_\mathrm{A}(d) = \sum_{i'} \nu_a(d \to i') \,, \tag{58.36a}$$

$$\nu_\mathrm{S}(d) = \sum_{f'} \nu_\mathrm{s}(d \to f') \,. \tag{58.36b}$$

Steady-State Distribution

For a steady-state distribution, the capture volume is

$$\frac{n_d^*}{n_\mathrm{e} N^+} = \frac{k_\mathrm{c}(d)}{\nu_\mathrm{A}(d) + \nu_\mathrm{S}(d)} \,. \tag{58.37}$$

Recombination Rate and Stabilization Probability

The recombination rate to channel f is

$$\hat{\alpha}_f = \sum_d \left(\frac{k_\mathrm{c}(d)\nu_\mathrm{s}(d \to f)}{\nu_\mathrm{A}(d) + \nu_\mathrm{S}(d)} \right) , \tag{58.38a}$$

and the rate to all product channels is

$$\hat{\alpha} = \sum_d \frac{k_\mathrm{c}(d)\nu_\mathrm{S}(d)}{\nu_\mathrm{A}(d) + \nu_\mathrm{S}(d)} \,. \tag{58.38b}$$

In the above, the quantities

$$P_f^\mathrm{S}(d) = \nu_\mathrm{s}(d \to f)/[\nu_\mathrm{A}(d) + \nu_S(d)] \,, \tag{58.39}$$

$$P^\mathrm{S}(d) = \nu_\mathrm{S}(d)/[\nu_\mathrm{A}(d) + \nu_\mathrm{S}(d)] \,, \tag{58.40}$$

represent the corresponding stabilization probabilities.

Macroscopic Detailed Balance and Saha Distribution

$$K_{di}(T) = \frac{\tilde{n}_d^*}{\tilde{n}_\mathrm{e}\tilde{N}^+} = \frac{k_\mathrm{c}(d)}{\nu_a(d \to i)} = k_\mathrm{c}(d)\tau_a(d \to i) \tag{58.41a}$$

$$= \frac{h^3}{(2\pi m_\mathrm{e} k_\mathrm{B} T)^{3/2}} \left(\frac{\omega(d)}{2\omega^+} \right) \exp\left(-E_{di}^*/k_\mathrm{B}T\right) , \tag{58.41b}$$

where E_{di}^* is the energy of superexcited neutral levels AB^{**} above that for ion level $\mathrm{AB}^+(i)$, and ω are the corresponding statistical weights.

Alternative Rate Formula

$$\hat{\alpha}_f = \sum_d K_{di} \left(\frac{\nu_a(d \to i)\nu_\mathrm{s}(d \to f)}{\nu_\mathrm{A}(d) + \nu_\mathrm{S}(d)} \right) . \tag{58.42}$$

Normalized Excited-State Distributions

$$\rho_d = n_d^*/\tilde{n}_d^* = \frac{\nu_a(d \to i)}{[\nu_\mathrm{A}(d) + \nu_\mathrm{S}(d)]} \,, \tag{58.43}$$

$$\hat{\alpha} = \sum_d k_\mathrm{c}(d) P^\mathrm{S}(d) = \sum_d K_{di}\rho_d \nu_\mathrm{S}(d) \tag{58.44a}$$

$$= \sum_d k_\mathrm{c}(d)[\rho_d \nu_\mathrm{S}(d)\tau_a(d \to i)] \,. \tag{58.44b}$$

Although equivalent, Eqs. (58.38a) and (58.42) are normally invoked for Eqs. (58.33) and (58.34), respectively, since $P^\mathrm{S} \le 1$ for DR, so that $\hat{\alpha}_\mathrm{DR} \to k_\mathrm{c}$; and $\nu_\mathrm{A} \gg \nu_S$ for DLR with $n \ll 50$ so that $\hat{\alpha} \to K_{di}\nu_\mathrm{s}$. For $n \gg 50$, $\nu_\mathrm{S} \gg \nu_\mathrm{A}$ and $\hat{\alpha} \to k_\mathrm{c}$. The above results Eqs. (58.38a) and (58.42) can also be derived from microscopic Breit–Wigner scattering theory for isolated (nonoverlapping) resonances.

58.3.2 Reactive Sphere Model: Three-Body Electron–Ion and Ion–Ion Recombination

Since the Coulomb attraction cannot support quasi-bound levels, three body electron–ion and ion–ion recombination

do not, in general, proceed via time-delayed resonances but rather by reactive (energy-reducing) collisions with the third body M. This is particularly effective for A–B separations $R \leq R_0$, as in the sequence

$$\mathrm{A} + \mathrm{B} \underset{\nu_\mathrm{d}}{\overset{k_\mathrm{c}}{\rightleftharpoons}} \mathrm{AB}^*(R \leq R_0) \,, \tag{58.45a}$$

$$\mathrm{AB}^*(R \leq R_0) + \mathrm{M} \underset{\nu_{-\mathrm{s}}}{\overset{\nu_\mathrm{s}}{\rightleftharpoons}} \mathrm{AB} + \mathrm{M} \,. \tag{58.45b}$$

In contrast to Eqs. (58.33) and (58.34), where the stabilization is irreversible, the forward step in Eq. (58.45b) is reversible. The sequence Eqs. (58.45a) and (58.45b) represents a closed system where thermodynamic equilibrium is eventually established.

Steady-State Distribution of *AB** Complex

$$n^* = \left(\frac{k_\mathrm{c}}{\nu_\mathrm{s} + \nu_d}\right) n_\mathrm{A}(t) n_\mathrm{B}(t) + \left(\frac{\nu_{-\mathrm{s}}}{\nu_\mathrm{s} + \nu_d}\right) n_\mathrm{s}(t) \,. \tag{58.46}$$

Saha and Boltzmann balances

$$\begin{aligned} &\text{Saha:} && \tilde{n}_\mathrm{A}\tilde{n}_\mathrm{B}k_\mathrm{c} &&= \tilde{n}^*\nu_d \,, \\ &\text{Boltzmann:} && \tilde{n}_\mathrm{s}\nu_{-\mathrm{s}} &&= \tilde{n}^*\nu_\mathrm{s} \,; \end{aligned} \tag{58.47}$$

$\tilde{n}^*$ is in Saha balance with reactant block C and in Boltzmann balance with product block S.

Normalized Distributions

$$\rho^* = \frac{n^*}{\tilde{n}^*} = P^\mathrm{D}\gamma_\mathrm{c}(t) + P^\mathrm{S}\gamma_\mathrm{s}(t) \,, \tag{58.48a}$$

$$\gamma_\mathrm{c}(t) = \frac{n_\mathrm{A}(t) n_\mathrm{B}(t)}{\tilde{n}_\mathrm{A}\tilde{n}_\mathrm{B}} \,, \quad \gamma_\mathrm{s}(t) = \frac{n_\mathrm{s}(t)}{\tilde{n}_\mathrm{s}} \,. \tag{58.48b}$$

Stabilization and Dissociation Probabilities

$$P^\mathrm{S} = \frac{\nu_\mathrm{s}}{(\nu_\mathrm{s} + \nu_\mathrm{d})}, \quad P^\mathrm{D} = \frac{\nu_\mathrm{d}}{(\nu_\mathrm{s} + \nu_\mathrm{d})} \,. \tag{58.49}$$

Time-Dependent Equations

$$\frac{\mathrm{d}n_\mathrm{c}}{\mathrm{d}t} = -k_\mathrm{c} P^\mathrm{S} \tilde{n}_\mathrm{A}\tilde{n}_\mathrm{B}[\gamma_\mathrm{c}(t) - \gamma_\mathrm{s}(t)] \,, \tag{58.50a}$$

$$\frac{\mathrm{d}n_\mathrm{s}}{\mathrm{d}t} = -\nu_{-\mathrm{s}} P^\mathrm{D} \tilde{n}_\mathrm{s}[\gamma_\mathrm{s}(t) - \gamma_\mathrm{c}(t)] \,, \tag{58.50b}$$

$$\frac{\mathrm{d}n_\mathrm{c}}{\mathrm{d}t} = -\hat{\alpha}_3 n_\mathrm{A}(t) n_\mathrm{B}(t) + k_\mathrm{d} n_\mathrm{s}(t) \,, \tag{58.51}$$

where the recombination rate coefficient (cm^3/s) and dissociation frequency are, respectively,

$$\hat{\alpha}_3 = k_\mathrm{c} P^\mathrm{S} = \frac{k_\mathrm{c}\nu_\mathrm{s}}{(\nu_\mathrm{s} + \nu_\mathrm{d})} \,, \tag{58.52}$$

$$k_\mathrm{d} = \nu_{-\mathrm{s}} P^\mathrm{D} = \frac{\nu_{-\mathrm{s}}\nu_\mathrm{d}}{(\nu_\mathrm{s} + \nu_\mathrm{d})} \,, \tag{58.53}$$

which also satisfy the macroscopic detailed balance relation

$$\hat{\alpha}_3 \tilde{n}_\mathrm{A}\tilde{n}_\mathrm{B} = k_\mathrm{d}\tilde{n}_\mathrm{s} \,. \tag{58.54}$$

Time-Independent Treatment

The rate $\hat{\alpha}_3$ given by the time-dependent treatment can also be deduced by viewing the recombination process as a source block C kept fully filled with dissociated species A and B maintained at equilibrium concentrations $\tilde{n}_\mathrm{A}, \tilde{n}_\mathrm{B}$ (i.e., $\gamma_\mathrm{c} = 1$) and draining at the rate $\hat{\alpha}_3 \tilde{n}_\mathrm{A}\tilde{n}_\mathrm{B}$ through a steady-state intermediate block $\mathcal{E}$ of excited levels into a fully absorbing sink block S of fully associated species AB kept fully depleted with $\gamma_\mathrm{s} = 0$, so that there is no backward redissociation from block S. The frequency k_d is deduced as if the reverse scenario, $\gamma_\mathrm{s} = 1$ and $\gamma_\mathrm{c} = 0$, holds. This picture uncouples $\hat{\alpha}$ and k_d and allows each coefficient to be calculated independently. Both dissociation (or ionization) and association (recombination) occur within block $\mathcal{E}$.

If $\gamma_\mathrm{c} = 1$ and $\gamma_\mathrm{s} = 0$, then

$$\rho^* = n^*/\tilde{n}^* = \nu_\mathrm{d}/(\nu_\mathrm{s} + \nu_\mathrm{d}) \,, \tag{58.55a}$$

$$K = \tilde{n}^*/\tilde{n}_\mathrm{A}\tilde{n}_\mathrm{B} = k_\mathrm{c}/\nu_\mathrm{d} = k_\mathrm{c}\tau_\mathrm{d} \,, \tag{58.55b}$$

$$P^\mathrm{S} = \nu_\mathrm{s}/(\nu_\mathrm{s} + \nu_\mathrm{d}) = \rho^*\nu_\mathrm{s}\tau_\mathrm{s} \,, \tag{58.55c}$$

and the recombination coefficient is

$$\hat{\alpha} = k_\mathrm{c} P^\mathrm{S} = k_\mathrm{c}(\rho^*\nu_\mathrm{s}\tau_\mathrm{d}) = K\rho^*\nu_\mathrm{s} \,. \tag{58.56}$$

Microscopic Generalization

From Eq. (58.206), the microscopic generalizations of rate in Eq. (58.52) and probability in Eq. (58.55c) are, respectively,

$$\hat{\alpha} = \overline{v} \int_0^\infty \varepsilon \mathrm{e}^{-\varepsilon} \mathrm{d}\varepsilon \int_0^{b_0} 2\pi b \, \mathrm{d}b P^\mathrm{S}(\varepsilon, b; R_0) \,, \tag{58.57a}$$

$$P^\mathrm{S}(\varepsilon, b; R_0) = \oint_{R_i}^{R_0} \rho_i(R) \nu_i^b(R) \, \mathrm{d}t \equiv \langle \rho\nu_\mathrm{s} \rangle \tau_\mathrm{d} \,, \tag{58.57b}$$

where $\rho_i(R) = n(\varepsilon, b; R)/\tilde{n}(\varepsilon, b; R)$; $\nu_i^{(b)}$ is the frequency Eq. (58.203a) of (A–B)–M continuum-bound collisional transitions at fixed A–B separation R, R_i is the pericenter of the orbit, $(i \equiv \varepsilon, b)$, and

$$b_0^2 = R_0^2[1 - V(R_0)/E], \quad \varepsilon = E/k_\mathrm{B}T \,, \tag{58.57c}$$

$$\hat{\alpha} \equiv k_\mathrm{c} \langle P^\mathrm{S} \rangle_{\varepsilon, b} \,, \quad \overline{v} = (8k_\mathrm{B}T/\pi \mathrm{M}_\mathrm{AB})^{1/2} \,, \tag{58.57d}$$

$$k_\mathrm{c} = \{\pi R_0^2[1 - V(R_0)/k_\mathrm{B}T]\overline{v}\} \,, \tag{58.57e}$$

where M_AB is the reduced mass of A and B.

Low Gas Densities

Here $\rho_i(R) = 1$ for $E > 0$,

$$P^\mathrm{S}(\varepsilon, b; R_0) = \oint_{R_i}^{R_0} \nu(t) \, \mathrm{d}t = \oint_{R_i}^{R_0} \mathrm{d}s/\lambda_i \,; \tag{58.58}$$

$\lambda_i = (N\sigma)^{-1}$ is the microscopic path length towards the (A–B)–M reactive collision with frequency $\nu = N v \sigma$. For λ_i

constant, the rate in Eq. (58.57a) reduces at low N to

$$\hat{\alpha} = (v\sigma_0 N)\int_0^{R_0}\left(1-\frac{V(R)}{k_B T}\right)4\pi R^2\,\mathrm{d}R\,, \qquad (58.59)$$

which is linear in the gas density N.

58.3.3 Working Formulae for Three-Body Collisional Recombination at Low Density

For three-body ion–ion collisional recombination of the form $A^+ + B^- + M$ in a gas at low density N, set $V(R) = -e^2/R$. Then Eq. (58.59) yields

$$\hat{\alpha}^{\mathrm{c}}(T) = \left(\frac{8k_B T}{\pi M_{AB}}\right)^{1/2}\frac{4}{3}\pi R_0^3\left(1+\frac{3}{2}\frac{R_e}{R_0}\right)(\sigma_0 N)\,, \qquad (58.60)$$

where $R_e = e^2/k_B T$, and the trapping radius R_0, determined by the classical variational method, is $0.41\,R_e$, in agreement with detailed calculation. The special cases are the following.

(a) $e^- + A^+ + e^-$

Here, $\sigma_0 = \frac{1}{9}\pi R_e^2$ for $(e^- - e^-)$ collisions for scattering angles $\theta \geq \pi/2$, so that

$$\hat{\alpha}^{\mathrm{c}}_{ee}(T) = 2.7\times 10^{-20}\left(\frac{300}{T}\right)^{4.5} n_e\,\mathrm{cm^3\,s^{-1}} \qquad (58.61)$$

in agreement with *Mansbach* and *Keck* [32].

(b) $A^+ + B^- + M$

Here, $\sigma_0\overline{v} \approx 10^{-9}\,\mathrm{cm^3\,s^{-1}}$, which is independent of T for polarization attraction. Then

$$\hat{\alpha}_3(T) = 2\times 10^{-25}\left(\frac{300}{T}\right)^{2.5} N\,\mathrm{cm^3\,s^{-1}}\,. \qquad (58.62)$$

(c) $e^- + A^+ + M$

Only a small fraction $\delta = 2m/M$ of the electron's energy is lost upon $(e^- - M)$ collision, so that Eq. (58.57a) for constant λ is modified to

$$\hat{\alpha}_{eM} = \sigma_0 N\int_0^{R_0} 4\pi R^2\,\mathrm{d}R\int_0^{E_m}\tilde{n}(R,E)v\,\mathrm{d}E \qquad (58.63a)$$

$$= \overline{v}_e\sigma_0 N\int_0^{R_0}4\pi R^2\,\mathrm{d}R\int_0^{\varepsilon_m}\left(1-\frac{V(R)}{E}\right)\varepsilon\,\mathrm{e}^{-\varepsilon}\,\mathrm{d}\varepsilon\,, \qquad (58.63b)$$

where $\varepsilon = E/k_B T$, and $E_m = \delta e^2/R = \varepsilon_m k_B T$ is the maximum energy for collisional trapping. Hence,

$$\hat{\alpha}_{eM}(T_e) = 4\pi\delta\left(\frac{8k_B T_e}{\pi m_e}\right)^{1/2} R_e^2 R_0[\sigma_0 N] \qquad (58.64a)$$

$$\approx \frac{10^{-26}}{M}\left(\frac{300}{T}\right)^{2.5} N\,\mathrm{cm^3\,s^{-1}}\,, \qquad (58.64b)$$

where the mass M of the gas atom is now in a.m.u. This result agrees with the energy diffusion result of *Pitaevskii* [33] when R_0 is taken as the Thomson radius $R_T = \frac{2}{3}R_e$.

58.3.4 Recombination Influenced by Diffusional Drift at High Gas Densities

Diffusional-Drift Current

The drift current of A^+ towards B^- in a gas under an A^+–B^- attractive potential $V(R)$ is

$$\boldsymbol{J}(R) = -D\nabla n(R) - \left[\frac{K}{e}\nabla V(R)\right]n(R) \qquad (58.65a)$$

$$= -\left(D\tilde{N}_A\tilde{N}_B\,\mathrm{e}^{-V(R)/k_B T}\frac{\partial\rho}{\partial R}\right)\hat{\boldsymbol{R}}\,. \qquad (58.65b)$$

Relative Diffusion and Mobility Coefficients

$$D = D_A + D_B\,,$$
$$K = K_A + K_B\,, \quad De = K(k_B T)\,, \qquad (58.66)$$

where the D_i and K_i are, respectively, the diffusion and mobility coefficients of species i in gas M.

Normalized Ion-Pair *R*-Distribution

$$\rho(R) = \frac{n(R)}{\tilde{N}_A\tilde{N}_B\exp[-V(R)/k_B T]}\,. \qquad (58.67)$$

Continuity Equations for Currents and Rates

$$\frac{\partial n}{\partial t} + \nabla\cdot\boldsymbol{J} = 0\,, \quad R\geq R_0\,, \qquad (58.68a)$$

$$\hat{\alpha}_{RN}(R_0)\rho(R_0) = \hat{\alpha}\rho(\infty)\,. \qquad (58.68b)$$

The rate of reaction for ion pairs with separations $R \leq R_0$ is $\alpha_{RN}(R_0)$. This is the recombination rate that would be obtained for a thermodynamic equilibrium distribution of ion pairs with $R \geq R_0$, i.e., for $\rho(R\geq R_0) = 1$.

Steady-State Rate of Recombination

$$\hat{\alpha}\tilde{N}_A\tilde{N}_B = \int_{R_0}^{\infty}\left(\frac{\partial n}{\partial t}\right)\mathrm{d}\boldsymbol{R} = -4\pi R_0^2 J(R_0)\,. \qquad (58.69)$$

Steady-State Solution

$$\rho(R) = \rho(\infty)\left(1-\frac{\hat{\alpha}}{\hat{\alpha}_{TR}(R)}\right), \quad R\geq R_0 \qquad (58.70a)$$

$$\rho(R_0) = \rho(\infty)[\hat{\alpha}/\hat{\alpha}_{RN}(R_0)]\,. \qquad (58.70b)$$

Recombination Rate

$$\hat{\alpha} = \frac{\hat{\alpha}_{\rm RN}(R_0)\hat{\alpha}_{\rm TR}(R_0)}{\hat{\alpha}_{\rm RN}(R_0) + \hat{\alpha}_{\rm TR}(R_0)} \tag{58.71a}$$

$$\to \begin{cases} \hat{\alpha}_{\rm RN}, & N \to 0 \\ \hat{\alpha}_{\rm TR}, & N \to \infty \, . \end{cases} \tag{58.71b}$$

Diffusional-Drift Transport Rate

$$\hat{\alpha}_{\rm TR}(R_0) = 4\pi D \left(\int_{R_0}^{\infty} \frac{{\rm e}^{V(R)/k_{\rm B}T}}{R^2} \, {\rm d}R \right)^{-1} . \tag{58.72}$$

With $V(R) = -e^2/R$,

$$\hat{\alpha}_{\rm TR}(R_0) = 4\pi K e [1 - \exp(-R_{\rm e}/R_0)]^{-1} \, , \tag{58.73}$$

where $R_{\rm e} = e^2/k_{\rm B}T$ provides a natural unit of length.

Langevin Rate

For $R_0 \ll R_{\rm e}$, the transport rate

$$\hat{\alpha}_{\rm TR} \to \hat{\alpha}_L = 4\pi K e \tag{58.74}$$

tends to the Langevin rate which varies as N^{-1}.

Reaction Rate

When R_0 is large enough that R_0-pairs are in (E, L^2) equilibrium Eq. (58.206),

$$\hat{\alpha}_{\rm RN}(R_0) = \overline{v} \int_0^{\infty} \varepsilon \, {\rm e}^{-\varepsilon} {\rm d}\varepsilon \int_0^{b_0} 2\pi b \, {\rm d}b P^{\rm S}(\varepsilon, b; R_0) \tag{58.75a}$$

$$\equiv \overline{v} \int_0^{\infty} \varepsilon \, {\rm e}^{-\varepsilon} \, {\rm d}\varepsilon \big[\pi b_0^2 P^{\rm S}(\varepsilon; R_0) \big] \tag{58.75b}$$

$$\equiv \overline{v} \pi b_{\rm max}^2 P^{\rm S}(R_0) \, , \tag{58.75c}$$

where

$$b_{\rm max}^2 = R_0^2 \left(1 - \frac{V(R_0)}{k_{\rm B}T} \right) , \tag{58.76}$$

and b_0 and ε are given by Eq. (58.57c) and $\overline{v}$ by Eq. (58.57d).

The probability $P^{\rm S}$ and its averages over b and (b, E) for reaction between pairs with $R \le R_0$ is determined in Eq. (58.75a–58.75c) from solutions of coupled master equations; $P^{\rm S}$ increases linearly with N initially and tends to unity at high N. The recombination rate in Eq. (58.71a) with Eq. (58.75a) and Eq. (58.73), therefore, increases linearly with N initially, reaches a maximum when $\hat{\alpha}_{\rm TR} \approx \hat{\alpha}_{\rm RN}$, and then decreases eventually as N^{-1}, in accord with Eq. (58.74).

Reaction Probability

The classical absorption solution of Eq. (58.196) is

$$P^{\rm S}(E, b; R_0) = 1 - \exp\left(- \oint_{R_i}^{R_0} \frac{{\rm d}s_i}{\lambda_i} \right) . \tag{58.77}$$

With the binary decomposition $\lambda_i^{-1} = \lambda_{i{\rm A}}^{-1} + \lambda_{i{\rm B}}^{-1}$,

$$P^{\rm S} = P_{\rm A} + P_{\rm B} - P_{\rm A} \, P_{\rm B} \, . \tag{58.78}$$

Exact b^2-Averaged Probability

With $V_{\rm c} = -e^2/R$ for the A^+–B^- interaction in Eq. (58.75b), and at low gas densities N,

$$P_{\rm A,B}(E, R_0) = \frac{\dfrac{4R_0}{3\lambda_{\rm A,B}} \left(1 - \dfrac{3V_{\rm c}(R_0)}{2E_i} \right)}{[1 - V_{\rm c}(R_0)/E_i]} \, , \tag{58.79}$$

appropriate for constant mean free path λ_i.

(E,b^2)-Averaged Probability

$P^{\rm S}(R_0)$ in Eq. (58.75c) at low gas density is

$$P_{\rm A,B}(R_0) = P_{\rm A,B}(E = k_{\rm B}T, R_0) \, . \tag{58.80}$$

Thomson Trapping Distance

When the kinetic energy gained from Coulomb attraction is assumed lost upon collision with third bodies, then bound (A, B) pairs are formed with $R \le R_{\rm T}$. Since $E = \frac{3}{2}k_{\rm B}T - e^2/R$, then

$$R_{\rm T} = \frac{2}{3} \left(\frac{e^2}{k_{\rm B}T} \right) = \frac{2}{3} R_{\rm e} \, . \tag{58.81}$$

Thomson Straight-Line Probability

The $E \to \infty$ limit of Eq. (58.77) is

$$P_{\rm A,B}^{\rm T}(b; R_{\rm T}) = 1 - \exp\big[-2\big(R_{\rm T}^2 - b^2\big)/\lambda_{\rm A,B} \big] \, . \tag{58.82}$$

The b^2-average is the Thomson probability

$$P_{\rm A,B}^{\rm T}(R_{\rm T}) = 1 - \frac{1}{2X^2} \big[1 - {\rm e}^{-2X}(1 + 2X) \big] \tag{58.83a}$$

for reaction of (A–B) pairs with $R \le R_{\rm T}$. As $N \to 0$

$$P_{\rm A,B}^{\rm T}(R_{\rm T}) \to \frac{4}{3} X \left(1 - \frac{3}{4} X + \frac{2}{5} X^2 - \frac{1}{6} X^3 + \cdots \right) \tag{58.83b}$$

and tends to unity at high N; $X = R_{\rm T}/\lambda_{\rm A,B} = N(\sigma_0 R_{\rm T})$. These probabilities have been generalized [34] to include hyperbolic and general trajectories.

Thomson Reaction Rate

$$\hat{\alpha}_{\rm T} = \pi R_{\rm T}^2 \overline{v} \big(P_{\rm A}^{\rm T} + P_{\rm B}^{\rm T} - P_{\rm A}^{\rm T} P_{\rm B}^{\rm T} \big)$$

$$\to \begin{cases} \frac{4}{3}\pi R_{\rm T}^3 \big(\lambda_{\rm A}^{-1} + \lambda_{\rm B}^{-1} \big), & N \to 0 \\ \pi R_{\rm T}^2 \overline{v}, & N \to \infty \, . \end{cases} \tag{58.84}$$

58.4 Zero-Range Methods

Zero-range methods refer to scattering models that make use of the scattering length to characterize the collision. Zero-range methods are used in ultracold collisions where the de Broglie wavelength of the atoms is much larger than the range of their interactions, and hence the scattering is well described by the S-wave scattering length, a.

The T-matrix element for S-wave scattering of two identical particles, mass m and energy $E = k^2/m$, is

$$T(k) = \frac{8\pi}{m} \frac{1}{k \cot \delta_0(k) - \imath k} , \tag{58.85}$$

where $\delta_0(k)$ is the S-wave phase shift. In general, one would solve numerically a couple-channel problem to compute the phase shifts for all the states of interest. In ultracold collisions, the low-energy effective range expansion of the S-wave phase shift can be utilized

$$k \cot \delta_0(k) = -1/a + \frac{1}{2} r_s k^2 + \cdots \tag{58.86}$$

to simplify the scattering calculation. The effective range expansion serves to define the scattering length a and the effective range r_s. See Sect. 47.5.5 and Eq. (47.46b) in this Handbook, and [35] for details on the scattering length and effective range. For the typical ultracold collision involving alkali atoms in specific hyperfine states, the van der Waals length, $\ell_{\rm vdW}$, and energy $E_{\rm vdW}$, provide natural length and energy scales, respectively

$$\ell_{\rm vdW} = (m C_6/\hbar^2)^{1/4} , \tag{58.87a}$$

$$E_{\rm vdW} = (m^3 C_6/\hbar^6)^{-1/2} , \tag{58.87b}$$

for atom of mass m and van der Waals constant C_6. For alkali atom collisions, the scattering lengths are [35]:

	^{6}Li(a_t)	^{85}Rb(a_s)	^{133}Cs(a_t)
$a(a_0)$	−2160	2800	2400

where the subscript s or t refer to singlet or triplet states, respectively.

Contrast these large values for alkali atom collisions with the much smaller values for $e^- + Rg$ atom collisions in Sect. 47.5.5 (Rg = He − Xe). See Table 1 of [26] for a more complete tabulation. The elastic scattering cross section for two bosonic atoms in the same spin state is

$$\sigma_{\rm elastic}(E) = \frac{8\pi a^2}{1 + m a^2 E} , \tag{58.88}$$

where a is the scattering length.

Shallow dimers

When $a > 0$, there is a single bound state with binding energy $E_D = 1/(ma^2)$, referred to as a shallow dimer state.

The three-body recombination rate α_s into a shallow dimer state is [26, 36]

$$\alpha_s = \frac{128\pi^2(4\pi - 3\sqrt{3})}{\sinh^2(\pi s_0) + \cosh^2(\pi s_0) \tan^2[s_0 \ln(a\kappa_\star) + \gamma]} \frac{\hbar a^4}{m} , \tag{58.89}$$

where $\kappa_\star$ is the wave number of the shallow dimer state $n_\star$, γ is a constant, and s_0 is the root of the transcendental equation

$$s_0 \cosh \frac{\pi s_0}{2} = \frac{8}{\sqrt{3}} \sinh \frac{\pi s_0}{6} , \tag{58.90}$$

with approximate numerical solution of $s_0 \sim 1.00624$. The phase constant γ has been computed in [37, 38] and is of order unity.

The three-body collision, at low energies in reaction Eq. (58.19), that results in the formation of dimers A_2 exhibits a universal property, wherein the spacing between adjacent energy levels of the dimer, $E_T^{(n)}$ follows an exponential scaling independent of system

$$E_T^{(n)} \longrightarrow (e^{-2\pi/s_0})^{n-n_\star} \frac{\hbar^2 \kappa_\star^2}{m} , \tag{58.91}$$

as $n \to \infty$, and where $\kappa_\star$ is the wave number associated with the dimer state labeled by the integer $n_\star$. The scaling relationship Eq. (58.91) was first described by *Efimov* [39, 40]. Further details on the universal scaling property Eq. (58.91) called the *Efimov effect* can be found in Sect. 60.6 of this Handbook, and [20, 25, 26, 41].

Deep dimers

Depending on the details of the short-range part of the dimer molecular potential, governed by the parameters a, $\kappa_\star$, and the inelasticity parameter $\eta_\star$, the dimer may support multiple states below threshold, called deep dimer states. See [26], and references therein, for a complete discussion of these parameters.

The three-body recombination rate α_d into a deep dimer state is [26]

$$\alpha_d = \frac{C_{\rm max} \cosh(\pi s_0) \sinh(\pi s_0) \cosh \eta_\star \sinh \eta_\star}{\sinh^2(\pi s_0 + \eta_\star) + \sin^2[s_0 \ln(a\kappa_\star) + \gamma]} \frac{\hbar a^4}{m} , \tag{58.92}$$

where $\eta_\star$ is the inelasticity parameter, and $C_{\rm max}$ is defined

$$C_{\rm max} = \frac{128\pi^2(4\pi - 3\sqrt{3})}{\sinh^2(\pi s_0)} , \tag{58.93}$$

while s_0 and γ retain their meaning as in Eq. (58.89).

Expressions for scattering lengths and effective ranges for shallow and deep dimers can be found in Sect. 60.6.

58.5 Hyperspherical Methods

Hyperspherical methods are techniques of solving the N-body Schrödinger equation where the coupled partial differential equations are reformulated in terms of hyperspherical coordinates. See Chap. 56 of this Handbook and [20] for details on hyperspherical methods.

d-dimensional coordinates [42]

$$R = \sqrt{x_1^2 + x_2^2 + x_3^2 + \cdots + x_d^2} \,. \tag{58.94}$$

$$\begin{aligned} x_d &= R\cos\alpha_{d-1} \,, \\ x_{d-1} &= R\sin\alpha_{d-1}\cos\alpha_{d-2} \,, \\ x_{d-2} &= R\sin\alpha_{d-1}\sin\alpha_{d-2}\cos\alpha_{d-3} \,, \\ &\cdots \\ x_2 &= R\prod_{j=1}^{d-1}\sin\alpha_j \,, \\ x_1 &= R\prod_{j=2}^{d-1}\sin\alpha_j\cos\alpha_1 \,, \end{aligned} \tag{58.95a}$$

where R is the hyperradius, x_i the coordinates of the particles, and α_j the corresponding hyperangles. The set Eq. (58.95a) is usually termed the canonical choice and have the ranges

$$0 \le \alpha_1 \le 2\pi, \quad 0 \le \alpha_i \le \pi, \quad i = 2, \ldots, d-1 \,. \tag{58.96}$$

The nonrelativistic kinetic energy operator is then separable

$$\hat{T} = T_R + \frac{\hbar^2 \Lambda^2}{2\mu R^2} \,, \tag{58.97a}$$

$$T_R = -\frac{\hbar^2}{2\mu}\frac{1}{R^{d-1}}R^{d-1}\frac{\partial}{\partial R} \,, \tag{58.97b}$$

where μ is the N-body reduced mass

$$\mu = (\mu_{12}\mu_{12,3}\cdots)^{1/(N-1)} \,, \tag{58.98}$$

and,

$$\mu_{12} = \frac{m_1 m_2}{m_1 + m_2} \,, \tag{58.99a}$$

$$\mu_{12,3} = \frac{(m_1 + m_2)m_3}{m_1 + m_2 + m_3} \,, \tag{58.99b}$$

the usual reduced masses, while Λ is the isotropic Casimir operator

$$\Lambda^2 = -\sum_{i>j}\Lambda_{ij}^2, \quad \Lambda_{ij} = x_i\frac{\partial}{\partial x_j} - x_j\frac{\partial}{\partial x_i} \,. \tag{58.100}$$

Three-particle case

$$R^2 = \rho_1^2 + \rho_2^2, \quad 0 \le R < \infty \,. \tag{58.101}$$

$$\vec{\rho}_1 = (\vec{r}_2 - \vec{r}_1)/\Delta \,, \tag{58.102a}$$

$$\vec{\rho}_2 = \Delta\left[\vec{r}_3 - \frac{m_1\vec{r}_1 + m_2\vec{r}_2}{m_1 + m_2}\right] \,, \tag{58.102b}$$

with,

$$\Delta^2 = \frac{1}{\mu}\frac{m_3(m_1 + m_2)}{m_1 + m_2 + m_3} \,, \tag{58.103a}$$

$$\mu^2 = \frac{m_1 m_2 m_3}{m_1 + m_2 + m_3} \,, \tag{58.103b}$$

for particles i with mass m_i and position vector $\vec{r}_i$, $i = 1$–3. The mass-scaled Jacobi coordinates, $\vec{\rho}_1$ and $\vec{\rho}_2$ determine the hyperangles θ and φ in the body frame x–y plane, yielding a rescaled Schrödinger equation for three identical particles

$$\left(-\frac{1}{2\mu}\frac{\partial^2}{\partial R^2} + \frac{15}{8\mu R^2} + \frac{\Lambda^2}{2\mu R^2} + V(R,\theta,\varphi)\right)\Psi_E = E\Psi_E \,, \tag{58.104}$$

where the full three-particle interaction potential V is expressed in terms of the hyperradius R and hyperangles θ and φ, and the angular momentum operator Λ is given in [20, equations (22–25)].

Coupled-channel expansion

$$\Psi_{Ev'} = \sum_{\nu}\frac{\Phi_\nu(R;\tilde{\omega})}{R^{(d-1)/2}}[f_{E\nu}(R)\delta_{\nu\nu'} - g_{E\nu}(R)K_{\nu\nu'}] \,, \tag{58.105}$$

where $f_{E\nu}(R)$ and $g_{E\nu}(R)$ are the regular and irregular radial functions, respectively; $K_{\nu\nu'}$ is the real symmetric reaction matrix, and $\tilde{\omega}$ represents the set of hyperangles, while d is the dimension.

The usual technique is to solve numerically the set of coupled equations and matching to linear combinations of regular and irregular functions at a large hyperradius R_0 to obtain the reaction matrix K.

58.5.1 Three-Body Recombination Rate (Identical Particles)

$$\alpha(E) = \frac{\hbar k}{\mu}\frac{192\pi^2}{k^5}\sum_{\nu'\nu}|S_{\nu'\nu}|^2 \,, \tag{58.106}$$

where $k = \sqrt{2\mu E/\hbar^2}$, and the S-matrix is determined from the reaction matrix using the standard expression Eq. (49.17). The sum includes all entrance channel ν three-body continuum states and exit channel ν' two-body bound states of A_2.

58.5.2 N-Body Recombination Rate (Identical Particles)

$$\alpha_N(E) = N!\frac{\hbar k}{\mu}\left(\frac{2\pi}{k}\right)^{d-1}\frac{\Gamma(d/2)}{2\pi^{d/2}}\sum_{\nu'\nu}|S_{\nu'\nu}|^2\,, \quad (58.107)$$

where $\Gamma(x)$ is the Gamma function and d is the dimension.

58.6 Field-Assisted Methods

Field-assisted methods is a general term to encompass techniques used to compute recombination rates in cases where the reaction is assisted by the application of an external field. Currently, the most commonly applied field is laser-assisted recombination Eq. (58.5) in studying the spectrum in high-order harmonic generation (HHG). See Sects. 78.3, 78.4 and 80.6 in this Handbook for further details on HHG.

Differential cross section [43]

$$\frac{d\sigma^R_{\rm len}}{d\Omega_k d\Omega_n} = \frac{4\pi^2\omega^3}{c^3 k}\left|a^{sc}_{\rm len}(k)\right|^2\,, \quad (58.108a)$$

$$\frac{d\sigma^R_{\rm acn}}{d\Omega_k d\Omega_n} = \frac{4\pi^2\omega}{c^3 k}\left|a^{sc}_{\rm acn}(k)\right|^2\,, \quad (58.108b)$$

where σ^R is the differential cross section for Eq. (58.5), the subscripts *len* and *acn* refer to the length and acceleration form of the matrix elements, respectively; ω is the angular frequency of the released photon, k the momentum of the recombining electron, Ω_n, Ω_k the corresponding solid angles, and c the speed of light.

He

$$a^{sc}_{\rm len}(k) = a_1 c_1 e^{\imath(\delta_1+\sigma_1)}\langle u_g r\rangle u^{sc}_{k1}\,, \quad (58.109a)$$

$$a^{sc}_{\rm acn}(k) = -a_1 c_1 Z_N e^{\imath(\delta_1+\sigma_1)}\langle u_g \frac{1}{r^2}\rangle u^{sc}_{k1}\,. \quad (58.109b)$$

Rg (Ar–Xe)

$$a^{sc}_{\rm len}(k) = a_0 c_0 e^{\imath(\delta_0+\sigma_0)}\langle u_g r\rangle u^{sc}_{k0} + a_2 c_2 e^{\imath(\delta_2+\sigma_2)}\langle u_g r\rangle u^{sc}_{k2} \quad (58.110a)$$

$$a^{sc}_{\rm acn}(k) = -a_0 c_0 Z_N e^{\imath(\delta_0+\sigma_0)}\langle u_g \frac{1}{r^2}\rangle u^{sc}_{k0} - a_2 c_2 Z_N e^{\imath(\delta_2+\sigma_2)}\langle u_g \frac{1}{r^2}\rangle u^{sc}_{k2}\,, \quad (58.110b)$$

where the constants a_ℓ and c_ℓ are defined

$$a_\ell = \frac{\imath^\ell}{2k}\sqrt{\frac{2\ell+1}{\pi}}\,, \quad (58.111a)$$

$$c_\ell = \langle Y^{m=0}_{\ell_g}\cos\theta\rangle Y^{m=0}_\ell\,, \quad (58.111b)$$

with Y^m_ℓ the spherical harmonics and Z_N the atomic number.

Detailed balance

$$\frac{d^2\sigma^R}{\omega^2 d\Omega_n d\Omega_k} = \frac{d^2\sigma^I}{k^2c^2 d\Omega_k d\Omega_n}\,, \quad (58.112)$$

where the superscripts R and I refer to recombination and ionization, respectively.

58.7 Dissociative Recombination

58.7.1 Curve-Crossing Mechanisms

Direct Process

Dissociative recombination (DR) for diatomic ions can occur via a crossing at R_X between the bound and repulsive potential energy curves $V^+(R)$ and $V_d(R)$ for AB^+ and AB^{**}, respectively. Here, DR involves the two-stage sequence

$$e^- + AB^+(v_i) \underset{\nu_a}{\overset{k_c}{\rightleftharpoons}} (AB^{**})_R \xrightarrow{\nu_d} A + B^*\,. \quad (58.113)$$

The first stage is dielectronic capture whereby the free electron of energy $\epsilon = V_d(R) - V^+(R)$ excites an electron of the diatomic ion AB^+ with internal separation R and is then resonantly captured by the ion, at rate k_c, to form a repulsive state d of the doubly excited molecule AB^{**}, which in turn can either autoionize at probability frequency ν_a, or else in the second stage, predissociate into various channels at probability frequency ν_d. This competition continues until the (electronically excited) neutral fragments accelerate past the crossing at R_X. Beyond R_X, the increasing energy of relative separation reduces the total electronic energy to such an extent that autoionization is essentially precluded, and the neutralization is then rendered permanent past the stabilization point R_X. This interpretation [44] has remained intact and robust in the current light of ab initio quantum chemistry and quantal scattering calculations for the simple diatomics (O_2^+, N_2^+, Ne_2^+, etc.). Mechanism Eq. (58.113) is termed the direct process, which, in terms of the macroscopic frequencies in Eq. (58.113), proceeds at the rate

$$\hat{\alpha} = k_c P_S = k_c[\nu_d/(\nu_a+\nu_d)]\,, \quad (58.114)$$

where P_S is probability for AB^* survival against autoionization from the initial capture at R_c to the crossing point R_X. Configuration mixing theories of this direct process are available in the quantal [45] and semiclassical-classical path formulations [46].

Indirect Process

In the three-stage sequence

$$e^- + AB^+(v_i^+) \to \left[AB^+(v_f) - e^-\right]_n \to (AB^{**})_d\,, \to A + B^* \quad (58.115)$$

the so-called indirect process [45] might contribute. Here, the accelerating electron loses energy by vibrational excitation $\left(v_i^+ \to v_f\right)$ of the ion and is then resonantly captured into a Rydberg orbital of the bound molecule AB^* in vibrational level v_f, which then interacts one way (via configuration mixing) with the doubly excited repulsive molecule AB^{**}. The capture initially proceeds via a small effect – vibronic coupling (the matrix element of the nuclear kinetic energy) induced by the breakdown of the Born–Oppenheimer approximation – at certain resonance energies $\varepsilon_n = E(v_f) - E\left(v_i^+\right)$ and, in the absence of the direct channel Eq. (58.113), would therefore be manifest by a series of characteristic very narrow Lorentz profiles in the cross section. Uncoupled from Eq. (58.113) the indirect process would augment the rate. Vibronic capture proceeds more easily when $v_f = v_i^+ + 1$, so that Rydberg states with $n \approx 7{-}9$ would be involved [for $H_2^+\left(v_i^+ = 0\right)$], so that the resulting longer periods of the Rydberg electron would permit changes in nuclear motion to compete with the electronic dissociation. Recombination then proceeds as in the second stage of Eq. (58.113), i.e., by electronic coupling to the dissociative state d at the crossing point. A multichannel quantum defect theory [47] has combined the direct and indirect mechanisms.

Interrupted Recombination

The process

$$\begin{gathered} e^- + AB^+(v_i) \underset{\nu_a}{\overset{k_c}{\rightleftharpoons}} (AB^{**})_d \overset{\nu_d}{\to} A + B^* \\ \nu_{nd} \uparrow\downarrow \nu_{dn} \\ \left[AB^+(v) - e^-\right]_n \end{gathered} \tag{58.116}$$

proceeds via the first (dielectronic capture) stage of Eq. (58.113) followed by a two-way electronic transition with frequency ν_{dn} and ν_{nd} between the d and n states. All (n, v) Rydberg states can be populated, particularly those in low n and high v since the electronic $d{-}n$ interaction varies as $n^{-1.5}$ with broad structure. Although the dissociation process proceeds here via a second-order effect (ν_{dn} and ν_{nd}), the electronic coupling may dominate the indirect vibronic capture and interrupt the recombination, in contrast to Eq. (58.115) which, as written in the one-way direction, feeds the recombination. Both dip and spike structure has been observed [48].

58.7.2 Quantal Cross Section

The cross section for direct dissociative recombination

$$e^- + AB^+\left(v_i^+\right) \rightleftharpoons \left(AB^{**}\right)_r \longrightarrow A + B^* \tag{58.117}$$

of electrons of energy ε, wavenumber k_e, and spin statistical weight 2, for a molecular ion $AB^+(v_i^+)$ of electronic statistical weight ω_{AB}^+ in vibrational level v_i^+ is

$$\begin{aligned} \sigma_{DR}(\varepsilon) &= \frac{\pi}{k_e^2}\left(\frac{\omega_{AB}^*}{2\omega^+}\right)\left|a_Q\right|^2 \\ &= \left(\frac{h^2}{8\pi m_e \varepsilon}\right)\left(\frac{\omega_{AB}^*}{2\omega^+}\right)\left|a_Q\right|^2 . \end{aligned} \tag{58.118}$$

Here, ω_{AB}^* is the electronic statistical weight of the dissociative neutral state of AB^* whose potential energy curve V_d crosses the corresponding potential energy curve V^+ of the ionic state. The transition T-matrix element for autoionization of AB^* embedded in the (moving) electronic continuum of $AB^+ + e^-$ is the quantal probability amplitude

$$a_Q(v) = 2\pi \int_0^\infty V_{d\varepsilon}^*(R)\left[\psi_v^{+*}(R)\psi_d(R)\right] dR \tag{58.119}$$

for autoionization. Here, ψ_v^+ and ψ_d are the nuclear bound and continuum vibrational wave functions for AB^+ and AB^*, respectively, while

$$\begin{aligned} V_{d\varepsilon}(R) &= \langle \phi_d | \mathcal{H}_{el}(\boldsymbol{r}, R(t)) | \phi_\varepsilon(\boldsymbol{r}, \boldsymbol{R}) \rangle_{\boldsymbol{r}, \hat{\epsilon}} \\ &= V_{\varepsilon d}^*(R) \end{aligned} \tag{58.120}$$

are the bound-continuum electronic matrix elements coupling the diabatic electronic bound state wave functions $\psi_d(\boldsymbol{r}, \boldsymbol{R})$ for AB^* with the electronic continuum state wave functions $\phi_\varepsilon(\boldsymbol{r}, \boldsymbol{R})$ for $AB^+ + e^-$. The matrix element is an average over electronic coordinates $\boldsymbol{r}$ and all directions $\hat{\epsilon}$ of the continuum electron. Both continuum electronic and vibrational wave functions are energy normalized (Sect. 58.11.3), and

$$\Gamma(R) = 2\pi |V_{d\varepsilon}^*(R)|^2 \tag{58.121}$$

is the energy width for autoionization at a given nuclear separation R. Given $\Gamma(R)$ from quantum chemistry codes, the problem reduces to evaluation of continuum vibrational wave functions in the presence of autoionization. The rate associated with a Maxwellian distribution of electrons at temperature T is

$$\hat{\alpha} = \overline{v}_e \int \varepsilon\, \sigma_{DR}(\varepsilon)\, e^{-\varepsilon/k_B T}\, d\varepsilon/(k_B T)^2 , \tag{58.122}$$

where $\overline{v}_e$ is the mean speed (Sect. 58.12).

Maximum Cross Section and Rate

Since the probability for recombination must remain less than unity, $\left|a_Q\right|^2 \leq 1$, so that the maximum cross section and

rates are

$$\sigma_{\mathrm{DR}}^{\max}(\varepsilon) = \frac{\pi}{k_{\mathrm{e}}^2}\left(\frac{\omega_{\mathrm{AB}}^*}{2\omega^+}\right) = \left(\frac{h^2}{8\pi m_{\mathrm{e}}\varepsilon}\right)(2\ell+1)\,, \quad (58.123)$$

where ω_{AB}^* has been replaced by $2(2\ell+1)\omega^+$ under the assumption that the captured electron is bound in a high-level Rydberg state of angular momentum ℓ, and

$$\hat{\alpha}_{\max}(T) = \overline{v}_{\mathrm{e}}\,\sigma_{\mathrm{DR}}^{\max}(\varepsilon = k_{\mathrm{B}}T) \quad (58.124a)$$

$$\approx 5\times10^{-7}\left(\frac{300}{T}\right)^{1/2}(2\ell+1)\,\mathrm{cm}^3/\mathrm{s}\,. \quad (58.124b)$$

Cross section maxima of $5(2\ell+1)(300/T)\times10^{-14}\,\mathrm{cm}^2$ are therefore possible, being consistent with the rate Eq. (58.124b).

First-Order Quantal Approximation

When the effect of autoionization on the continuum vibrational wave function $\psi_d(R)$ for AB^* is ignored, then a first-order undistorted approximation to the quantal amplitude Eq. (58.119) is

$$T_{\mathrm{B}}(v^+) = 2\pi\int_0^\infty V_{d\varepsilon}^*(R)\left[\psi_v^{+*}(R)\psi_d^{(0)}(R)\right]\mathrm{d}R\,, \quad (58.125)$$

where $\psi_d^{(0)}$ is ψ_d in the absence of the back reaction of autoionization. Under this assumption, Eq. (58.118) reduces to

$$\sigma_{\mathrm{c}}(\varepsilon, v^+) = \frac{\pi}{k_{\mathrm{e}}^2}\left(\frac{\omega_{\mathrm{AB}}^*}{2\omega^+}\right)\left|T_{\mathrm{B}}(v^+)\right|^2\,, \quad (58.126)$$

which is then the cross section for initial electron capture since autoionization has been precluded. Although the Born T-matrix Eq. (58.125) violates unitarity, the capture cross section Eq. (58.126) must remain less than the maximum value

$$\sigma_{\mathrm{c}}^{\max} = \frac{\pi}{k_{\mathrm{e}}^2}\left(\frac{\omega_{\mathrm{AB}}^*}{2\omega^+}\right) = \left(\frac{h^2}{8\pi m_{\mathrm{e}}\varepsilon}\right)\left(\frac{\omega_{\mathrm{AB}}^*}{2\omega^+}\right)\,, \quad (58.127)$$

since $|a_Q|^2 \le 1$. So as to acknowledge after the fact the effect of autoionization, assumed small, and neglected by Eq. (58.125), the DR cross section can be approximated as

$$\sigma_{\mathrm{DR}}(\varepsilon, v^+) = \sigma_{\mathrm{c}}(\varepsilon, v^+)P_{\mathrm{S}}\,, \quad (58.128)$$

where P_{S} is the probability of survival against autoionization on the V_d curve until stabilization takes place at some crossing point R_X.

Approximate Capture Cross Section

With the energy-normalized Winans–Stückelberg vibrational wave function

$$\psi_d^{(0)}(R) = |V_d'(R)|^{-1/2}\delta(R-R_{\mathrm{c}})\,, \quad (58.129)$$

where R_{c} is the classical turning point for $(\mathrm{A}-\mathrm{B}^*)$ relative motion, Eq. (58.126) reduces to

$$\sigma_{\mathrm{c}}(\varepsilon, v^+) = \frac{\pi}{k_{\mathrm{e}}^2}\left(\frac{\omega_{\mathrm{AB}}^*}{2\omega^+}\right)[2\pi\Gamma(R_{\mathrm{c}})]\left\{\frac{|\psi_v^+(R_{\mathrm{c}})|^2}{|V_d'(R_{\mathrm{c}})|}\right\}\,, \quad (58.130)$$

where the term inside the braces in Eq. (58.130) is the effective Franck–Condon factor.

Six Approximate Stabilization Probabilities

(1)

A unitarized T-matrix is

$$T = \frac{T_{\mathrm{B}}}{1+\left|\frac{1}{2}T_{\mathrm{B}}\right|^2}\,, \quad (58.131)$$

so that $P_{\mathrm{S}} = |T|^2/|T_{\mathrm{B}}|^2$ to give

$$P_{\mathrm{S}}(\text{low }\varepsilon) = \left(1+\frac{1}{4}|T_{\mathrm{B}}|^2\right)^{-2} = \left\{1+\pi^2\left|\int_0^\infty V_{d\varepsilon}^*(R)\left[\psi_v^{+*}(R)\psi_d^{(0)}(R)\right]\mathrm{d}r\right|^2\right\}^{-2}\,, \quad (58.132a)$$

which is valid at low ε when only one vibrational level v^+, i.e., the initial level of the ion is repopulated by autoionization.

(2)

At higher ε, when population of many other ionic levels v_f^+ occurs, then

$$P_{\mathrm{S}}(\varepsilon) = \left[1+\frac{1}{4}\sum_f\left|T_{\mathrm{B}}(v_f^+)\right|^2\right]^{-2}\,, \quad (58.132b)$$

where the summation is over all the open vibrational levels v_f^+ of the ion. When no intermediate Rydberg $\mathrm{AB}^*(v)$ states are energy resonant with the initial $\mathrm{e}^- + \mathrm{AB}^+(v^+)$ state, i.e., coupling with the indirect mechanism is neglected, then Eq. (58.128), with Eq. (58.132b), is the direct DR cross section normally calculated.

(3)
In the high-ε limit, when an infinite number of v_f^+ levels are populated following autoionization, the survival probability, with the aid of closure, is then

$$P_S = \left[1 + \pi^2 \int_{R_c}^{R_X} |V^*_{d\varepsilon}(R)|^2 \left|\psi_d^{(0)}(R)\right|^2 \mathrm{d}R\right]^{-2} . \quad (58.133)$$

(4)
On adopting in Eq. (58.133) the JWKB semiclassical wave function for $\psi_d^{(0)}$,

$$P_S(\text{high } \varepsilon) = \left[1 + \frac{1}{2\hbar}\int_{R_c}^{R_X} \frac{\Gamma(R)}{v(R)}\,\mathrm{d}R\right]^{-2} = \left[1 + \frac{1}{2}\int_{t_c}^{t_X} \nu_a(t)\,\mathrm{d}t\right]^{-2} , \quad (58.134)$$

where $v(R)$ is the local radial speed of A−B relative motion, and where the frequency $\nu_a(t)$ of autoionization is $\Gamma/\hbar$.

(5)
A classical path local approximation for P_S yields

$$P_S = \exp\left(-\int_{t_c}^{t_X} \nu_a(t)\,\mathrm{d}t\right) , \quad (58.135)$$

which agrees to first order for small ν with the expansion of Eq. (58.134).

(6)
A partitioning of Eq. (58.113) yields

$$P_S = \nu_d/(\nu_a + \nu_d) = (1 + \nu_a\tau_d)^{-1} , \quad (58.136)$$

on adopting macroscopic averaged frequencies ν_i and associated lifetimes $\tau_i = \nu_i^{-1}$. The six survival probabilities in Eqs. (58.132a), (58.132b), (58.132a), (58.133)–(58.136) are all suitable for use in the DR cross section Eq. (58.128).

58.7.3 Noncrossing Mechanism

The dissociative recombination (DR) processes

$$\begin{aligned} e^- + H_3^+ &\to H_2 + H \\ &\to H + H + H \end{aligned} \quad (58.137)$$

at low electron energy ε, and

$$e^- + HeH^+ \to He + H \quad (n = 2) \quad (58.138)$$

have spurred renewed theoretical interest because they both proceed at respective rates of $(2\times10^{-7}$ to $2\times10^{-8})$ cm^3 s^{-1} and 10^{-8} cm^3 s^{-1} at 300 K. Such rates are generally associated with the direct DR, which involves favorable curve crossings between the potential energy surfaces, $V^+(R)$ and $V_d(R)$ for the ion AB^+ and neutral dissociative AB^{**} states. The difficulty with Eqs. (58.137) and (58.138) is that there are no such curve crossings, except at $\varepsilon \geq 8$ eV for Eq. (58.137). In this instance, the previous standard theories would support only extremely small rates when electronic resonant conditions do not prevail at thermal energies. Theories [49–53] have been developed for application to processes such as Eq. (58.137).

58.8 Mutual Neutralization

$$A^+ + B^- \to A + B . \quad (58.139)$$

Diabatic potentials
$V_i^{(0)}(R)$ and $V_f^{(0)}(R)$ for initial (ionic) and final (covalent) states are diagonal elements of

$$V_{if}(R) = \langle \Psi_i(\boldsymbol{r}, \boldsymbol{R})|\mathcal{H}_{el}(\boldsymbol{r}, \boldsymbol{R})|\Psi_f(\boldsymbol{r}, \boldsymbol{R})\rangle_{\boldsymbol{r}} , \quad (58.140)$$

where $\Psi_{i,f}$ are diabatic states, and $\mathcal{H}_{el}$ is the electronic Hamiltonian at fixed internuclear distance R.

Adiabatic potentials for a two-state system

$$V^{\pm}(R) = V_0(R) \pm \left[\Delta^2(R) + \left|V_{if}(R)\right|^2\right]^{1/2} , \quad (58.141a)$$

$$V_0(R) = \frac{1}{2}\left[V_i^{(0)}(R) + V_f^{(0)}(R)\right] , \quad (58.141b)$$

$$\Delta(R) = \left[V_i^{(0)}(R) - V_f^{(0)}(R)\right] . \quad (58.141c)$$

For a single crossing of diabatic potentials at R_X, $V_i^{(0)}(R_X) = V_f^{(0)}(R_X)$ and the adiabatic potentials at R_X are

$$V^{\pm}(R_X) = V_i^{(0)}(R_X) \pm V_{if}(R_X) , \quad (58.142)$$

with energy separation $2V_{if}(R_X)$.

58.8.1 Landau–Zener Probability for Single Crossing at R_X

On assuming $\Delta(R) = (R - R_X)\Delta'(R_X)$, where $\Delta'(R) = \mathrm{d}\Delta(R)/\mathrm{d}R$, the probability for single crossing is

$$P_{if}(R_X) = \exp[\eta(R_X)/v_X(b)] , \quad (58.143a)$$

$$\eta(R_X) = \left(\frac{2\pi}{\hbar}\right)\frac{\left|V_{if}(R_X)\right|^2}{\Delta'(R_X)} , \quad (58.143b)$$

$$v_X(b) = \left[1 - V_i^{(0)}(R_X)/E - b^2/R_X^2\right]^{1/2} . \quad (58.143c)$$

Overall Charge-Transfer Probability

From the incoming and outgoing legs of the trajectory,

$$P^X(E) = 2P_{if}(1 - P_{if}) . \quad (58.144)$$

58.8.2 Cross Section and Rate Coefficient for Mutual Neutralization

$$\begin{aligned}\sigma_{\rm M}(E) &= 4\pi \int_0^{b_X} P_{if}(1 - P_{if}) b\, {\rm d}b \\ &= \pi b_X^2 P_{\rm M} , \\ \pi b_X^2 &= \pi\left(1 - \frac{V_i^{(0)}(R_X)}{E}\right) R_X^2 \\ &= \pi\left(1 + \frac{14.4}{R_X(\text{Å})E(\text{eV})}\right) R_X^2 ; \end{aligned} \quad (58.145a)$$

$P_{\rm M}$ is the b^2-averaged probability Eq. (58.144) for charge-transfer reaction within a sphere of radius R_X.

The rate is

$$\hat{\alpha}_{\rm M} = (8k_{\rm B}T/\pi {\rm M}_{\rm AB})^{1/2} \int_0^\infty \epsilon \sigma_{\rm M}(\epsilon)\, {\rm e}^{-\epsilon} {\rm d}\epsilon , \quad (58.146)$$

where $\epsilon = E/k_{\rm B}T$.

58.9 One-Way Microscopic Equilibrium Current, Flux, and Pair Distributions

All quantities on the RHS in the Cases (a)–(e) below are to be multiplied by $\tilde{N}_{\rm A}\tilde{N}_{\rm B}[\omega_{\rm AB}/\omega_{\rm A}\omega_{\rm B}]$, where the ω_i denote the statistical weights of species i that are not included by the density of states associated with the E, L^2 orbital degrees of freedom.

Case (a)

$(i \equiv \boldsymbol{R},\ E,\ L^2)$.

$$\begin{aligned}&\text{Current: } j_i^{\pm}(R) = n^{\pm}(\boldsymbol{R}, E, L^2) v_{\rm R} \equiv n_i^{\pm} v_{\rm R} . \\ &\text{Flux: } 4\pi R^2 j_i^{\pm}(R){\rm d}E{\rm d}L^2 = \frac{4\pi^2 {\rm e}^{-E/k_{\rm B}T}}{(2\pi {\rm M}_{\rm AB} k_{\rm B}T)^{3/2}} {\rm d}E{\rm d}L^2 .\end{aligned} \quad (58.147)$$

This flux is independent of R. For dissociated pairs $E > 0$,

$$4\pi R^2 j_i^{\pm}(R){\rm d}E{\rm d}L^2 = [\overline{v}\varepsilon\, {\rm e}^{-\varepsilon}{\rm d}\varepsilon][2\pi b{\rm d}b] . \quad (58.148)$$

$(\boldsymbol{R}, E, L^2)$-distribution

$$\begin{aligned}&n(\boldsymbol{R}, E, L^2){\rm d}\boldsymbol{R}{\rm d}E{\rm d}L^2 \\ &= \frac{(8\pi^2/v_{\rm R})\, {\rm e}^{-E/k_{\rm B}T}}{(2\pi {\rm M}_{\rm AB}k_{\rm B}T)^{3/2}} \left(\frac{{\rm d}\boldsymbol{R}}{4\pi R^2}\right) {\rm d}E{\rm d}L^2 .\end{aligned} \quad (58.149)$$

Case (b)

$(i \equiv \boldsymbol{R},\ E,\ L^2)$-integrated quantities.

$$\text{Current: } j_i^{\pm}(R) = \frac{1}{2} v n^{\pm}(\boldsymbol{R}, E) \equiv \frac{1}{2} v n_i^{\pm} . \quad (58.150)$$

$$\text{Flux:} \quad 4\pi R^2 j_i^{\pm}(R){\rm d}E = [\overline{v}\varepsilon\, {\rm e}^{-\varepsilon}{\rm d}\varepsilon]\pi b_0^2 , \quad (58.151a)$$

$$\pi b_0^2 = \pi R^2[1 - V(R)/E] . \quad (58.151b)$$

$(\boldsymbol{R}, E)$-Distribution:

$$\begin{aligned}&n(\boldsymbol{R}, E){\rm d}\boldsymbol{R}{\rm d}E \\ &= \frac{2}{\sqrt{\pi}}\left[\frac{E - V(R)}{k_{\rm B}T}\right]^{1/2} {\rm e}^{-\varepsilon}{\rm d}\varepsilon{\rm d}\boldsymbol{R} \\ &\equiv G_{\rm MB}(E, R){\rm d}\boldsymbol{R} ,\end{aligned} \quad (58.151c)$$

which defines the Maxwell–Boltzmann velocity distribution $G_{\rm MB}$ in the presence of the field $V(R)$.

Case (c)

(E, L^2)-integrated quantities.

$$\text{Current:} \quad j^{\pm}(R) = \frac{1}{4}\overline{v}\, {\rm e}^{-V(R)/k_{\rm B}T} . \quad (58.152)$$

$$\text{Flux:} \quad 4\pi R^2 j^{\pm}(R) = \pi R^2 \overline{v}\, {\rm e}^{-V(R)/k_{\rm B}T} . \quad (58.153)$$

$$\text{Distribution:} \quad n(R) = {\rm e}^{-V(R)/k_{\rm B}T} . \quad (58.154)$$

When E-integration is only over dissociated states ($E > 0$), the above quantities are

$$j_d^{\pm}(R) = \frac{1}{4}\overline{v}[1 - V(R)/k_{\rm B}T] , \quad (58.155)$$

$$4\pi R^2 j_d^{\pm}(R) = \pi R^2\left(1 - \frac{V(R)}{k_{\rm B}T}\right)\overline{v} \equiv \pi b_{\rm max}^2 \overline{v} , \quad (58.156)$$

$$n(R) = [1 - V(R)/k_{\rm B}T] . \quad (58.157)$$

Case (d)

(E, L^2)-distribution. For bound levels

$$n(E, L^2){\rm d}E{\rm d}L^2 = \frac{4\pi^2 \tau_{\rm R}(E, L)}{(2\pi {\rm M}_{\rm AB}k_{\rm B}T)^{3/2}} {\rm e}^{-E/k_{\rm B}T}{\rm d}E{\rm d}L^2 , \quad (58.158)$$

where $\tau_{\rm R} = \oint {\rm d}t = (\partial J_{\rm R}/\partial E)$ is the period for bounded radial motion of energy E and radial action $J_{\rm R}(E, L) = {\rm M}_{\rm AB} \oint v_{\rm R}{\rm d}R$.

Case (e)
E-distribution. For bound levels

$$n(E)\mathrm{d}E = \frac{2\mathrm{e}^{-\varepsilon}}{\sqrt{\pi}}\mathrm{d}\varepsilon \int_0^{R_\mathrm{A}} \left(\frac{E-V}{k_\mathrm{B}T}\right)^{1/2} \mathrm{d}\boldsymbol{R}\ , \tag{58.159}$$

where R_A is the turning point $E = V(R_\mathrm{A})$.

Example
For electron–ion bounded motion, $V(R) = -Ze^2/R$, $R_\mathrm{A} = Ze^2/|E|$, $R_\mathrm{e} = Ze^2/k_\mathrm{B}T$, $\varepsilon = E/k_\mathrm{B}T$. Then $\tau_\mathrm{R} = 2\pi(m/Ze^2)^{1/2}(R_\mathrm{A}/2)^{3/2}$,

$$\int_0^{R_\mathrm{A}} \left(\frac{R_\mathrm{e}}{R} - |\varepsilon|\right)^{1/2} \mathrm{d}\boldsymbol{R} = \frac{\pi^2}{4} R_\mathrm{A}^{5/2} R_\mathrm{e}^{1/2}\ , \tag{58.160}$$

and

$$n^s(E)\mathrm{d}E = \left(\frac{2\mathrm{e}^{-\varepsilon}}{\sqrt{\pi}}\, d\varepsilon\right)\frac{\pi^2}{4} R_\mathrm{A}^{5/2} R_\mathrm{e}^{1/2} \tag{58.161}$$

$$= \left(\frac{2\mathrm{e}^{-\varepsilon}}{\sqrt{\pi}}\mathrm{d}\varepsilon\right)\left(\frac{\pi^2 R_\mathrm{e}^3}{4|\varepsilon|^{5/2}}\right)\ . \tag{58.162}$$

For closely spaced levels in a hydrogenic $\mathrm{e}^- - \mathrm{A}^{Z+}$ system,

$$n^s(p,\ell) = n\big(E, L^2\big)\left(\frac{\mathrm{d}E}{\mathrm{d}p}\right)\left(\frac{\mathrm{d}L^2}{\mathrm{d}\ell}\right)\ , \tag{58.163a}$$

$$n^s(p) = n(E)\left(\frac{\mathrm{d}E}{\mathrm{d}p}\right)\ . \tag{58.163b}$$

Using $E = -\big(2p^2\big)^{-1}\big(Z^2e^2/a_0\big)$ and $L^2 = (\ell + 1/2)^2\hbar^2$ for level (p,ℓ) then

$$\tau_\mathrm{R}(E,L)\frac{\mathrm{d}E}{\mathrm{d}p}\left(\frac{\mathrm{d}L^2}{\mathrm{d}\ell}\right) = \left(\frac{\mathrm{d}J_\mathrm{R}}{\mathrm{d}p}\right)\left(\frac{\mathrm{d}L^2}{\mathrm{d}\ell}\right) \tag{58.164}$$

$$= h\big((2\ell+1)\hbar^2\big)\ , \tag{58.165}$$

$$\frac{n^s(p,\ell)}{n_\mathrm{e}N^+} = \frac{2(2\ell+1)}{2\omega_\mathrm{A}^+}\frac{h^3}{(2\pi m_\mathrm{e}k_\mathrm{B}T)^{3/2}}\mathrm{e}^{I_p/k_\mathrm{B}T}\ , \tag{58.166a}$$

$$\frac{n^s(p)}{n_\mathrm{e}N^+} = \frac{2p^2}{2\omega_\mathrm{A}^+}\frac{h^3}{(2\pi m_\mathrm{e}k_\mathrm{B}T)^{3/2}}\mathrm{e}^{I_p/k_\mathrm{B}T}\ , \tag{58.166b}$$

in agreement with the Saha ionization formula Eq. (58.28), where N^+ is the equilibrium concentration of A^{Z+} ions in their ground electronic states. The spin statistical weights are $\omega_{e\mathrm{A}} = \omega_\mathrm{e} = 2$.

Notation:

$\mathrm{M_{AB}}$	reduced mass $\mathrm{M_A\,M_B/(M_A + M_B)}$
R	internal separation of A–B
E	orbital energy $\frac{1}{2}\mathrm{M}v^2 + V(R)$
L	orbital angular momentum
L^2	$2\mathrm{M}Eb^2$ for $E > 0$
v_R	radial speed $\lvert\dot{R}\rvert$
$\overline{v}$	mean relative speed $(8kT/\pi\mathrm{M_{AB}})^{1/2}$
ε	normalized energy $E/k_\mathrm{B}T$
n_i	pair distribution function $n_i^+ + n_i^-$
$n_i^\pm$	component of n_i with $\dot{R} > 0$ (+) and $\dot{R} < 0$ (−).

58.10 Microscopic Methods for Termolecular Ion–Ion Recombination

At low gas density, the basic process

$$\mathrm{A}^+ + \mathrm{B}^- + \mathrm{M} \to \mathrm{AB} + \mathrm{M} \tag{58.167}$$

is characterized by nonequilibrium with respect to E. Dissociated and bound A^+–B^- ion pairs are in equilibrium with respect to their separation R, but bound pairs are not in E-equilibrium with each other; L^2-equilibrium can be assumed for ion–ion recombination but not for ion–atom association reactions.

At higher gas densities N, there is nonequilibrium in the ion-pair distributions with respect to R, E, and L^2. In the limit of high N, there is only nonequilibrium with respect to R. See [54] for full details.

58.10.1 Time-Dependent Method: Low Gas Density

Energy levels E_i of A^+–B^- pairs are so close that they form a quasi continuum with a nonequilibrium distribution over E_i determined by the master equation

$$\frac{\mathrm{d}n_i(t)}{\mathrm{d}t} = \int_{-D}^{\infty} \big(n_i v_{if} - n_f v_{fi}\big)\mathrm{d}E_f\ , \tag{58.168}$$

where $n_i\mathrm{d}E_i$ is the number density of pairs in the interval $\mathrm{d}E_i$ about E_i, and $v_{if}\mathrm{d}E_f$ is the frequency of i-pair collisions with M that change the i-pair orbital energy from E_i to between E_f and $E_f + \mathrm{d}E_f$. The greatest binding energy of the A^+–B^- pair is D.

Association Rate

$$R^\mathrm{A}(t) = \int_{-D}^{\infty} P_i^\mathrm{S}\left(\frac{\mathrm{d}n_i}{\mathrm{d}t}\right)\mathrm{d}E_i \tag{58.169a}$$

$$= \hat{\alpha}N_\mathrm{A}(t)N_\mathrm{B}(t) - kn_\mathrm{s}(t)\ , \tag{58.169b}$$

where P_i^{S} is the probability for collisional stabilization (recombination) of i-pairs via a sequence of energy changing collisions with M. The coefficients for $C \to S$ recombination out of the C-block with ion concentrations $N_{\mathrm{A}}(t)$, $N_{\mathrm{B}}(t)$ (in cm^{-3}) into the S block of total ion-pair concentrations $n_{\mathrm{s}}(t)$ and for $S \to C$ dissociation are $\hat{\alpha}$ ($\mathrm{cm}^3\,\mathrm{s}^{-1}$) and $k(\mathrm{s}^{-1})$, respectively.

One-Way Equilibrium Collisional Rate and Detailed Balance

$$\mathrm{C}_{if} = \tilde{n}_i \nu_{if} = \tilde{n}_f \nu_{fi} = \mathrm{C}_{fi} \ , \tag{58.170}$$

where the tilde denotes equilibrium (Saha) distributions.

Normalized Distribution Functions

$$\gamma_i(t) = n_i(t)/\tilde{n}_i^{\mathrm{S}} \ , \quad \gamma_{\mathrm{s}}(t) = n_s(t)/\tilde{n}_{\mathrm{s}}^{\mathrm{B}}(t) \ , \tag{58.171}$$

$$\gamma_{\mathrm{c}}(t) = N_{\mathrm{A}}(t) N_{\mathrm{B}}(t)/\tilde{N}_{\mathrm{A}}\tilde{N}_{\mathrm{B}} \ , \tag{58.172}$$

where $\tilde{n}_i^{\mathrm{S}}$ and $\tilde{n}^{\mathrm{B}}$ are the Saha and Boltzmann distributions.

Master Equation for $\gamma_i(t)$

$$\frac{\mathrm{d}\gamma_i(t)}{\mathrm{d}t} = -\int_{-D}^{\infty} \left[\gamma_i(t) - \gamma_f(t)\right] \nu_{if} \mathrm{d}E_f \ . \tag{58.173}$$

Quasi-Steady State (QSS) Reduction

Set

$$\gamma_i(t) = P_i^{\mathrm{D}} \gamma_{\mathrm{c}}(t) + P_i^{\mathrm{S}} \gamma_{\mathrm{s}}(t) \overset{t\to\infty}{\longrightarrow} 1 \ , \tag{58.174}$$

where P_i^{D} and P_i^{S} are the respective time-independent portions of the normalized distribution γ_i, which originate, respectively, from blocks C and S. The energy separation between the C and S blocks is so large that $P_i^{\mathrm{S}} = 0$ ($E_i \geq 0$, C block), $P_i^{\mathrm{S}} \leq 1$ ($0 > E_i \geq -S$, $\mathcal{E}$ block), and $P_i^{\mathrm{S}} = 1$ ($-S \geq E_i \geq -D$, S block). Since $P_i^{\mathrm{S}} + P_i^{\mathrm{D}} = 1$, then

$$\frac{\mathrm{d}\gamma_i(t)}{\mathrm{d}t} = -[\gamma_{\mathrm{c}}(t) - \gamma_{\mathrm{s}}(t)] \int_{-D}^{\infty} \left(P_i^{\mathrm{D}} - P_f^{\mathrm{D}}\right) \mathrm{C}_{if} \mathrm{d}E_f \ . \tag{58.175}$$

Recombination and Dissociation Coefficients

Equation (58.174) in Eq. (58.169a) enables the recombination rate in Eq. (58.169b) to be written as

$$\hat{\alpha}\tilde{N}_{\mathrm{A}}\tilde{N}_{\mathrm{B}} = \int_{-D}^{\infty} P_i^{\mathrm{D}} \mathrm{d}E_i \int_{-D}^{\infty} \left(P_i^{\mathrm{D}} - P_f^{\mathrm{D}}\right) \mathrm{C}_{if} \mathrm{d}E_f \ . \tag{58.176}$$

The QSS condition ($\mathrm{d}n_i/\mathrm{d}t = 0$ in block $\mathcal{E}$) is then

$$P_i^{\mathrm{D}} \int_{-D}^{\infty} \nu_{if} \mathrm{d}E_f = \int_{-D}^{E} \nu_{if} P_f^{\mathrm{D}} \mathrm{d}E_f \ , \tag{58.177}$$

which involves only time-independent quantities. Under QSS, Eq. (58.176) reduces to the net downward current across bound level $-E$,

$$\hat{\alpha}\tilde{N}_{\mathrm{A}}\tilde{N}_{\mathrm{B}} = \int_{-E}^{\infty} \mathrm{d}E_i \int_{-D}^{-E} \left(P_i^{\mathrm{D}} - P_f^{\mathrm{D}}\right) \mathrm{C}_{if} \mathrm{d}E_f \ , \tag{58.178}$$

which is independent of the energy level ($-E$) in the range $0 \geq -E \geq -S$ of block $\mathcal{E}$.

The dissociation frequency k in Eq. (58.169b) is

$$k\tilde{n}_{\mathrm{s}} = \int_{-D}^{-E} \mathrm{d}E_i \int_{-E}^{\infty} \left(P_i^{\mathrm{S}} - P_f^{\mathrm{S}}\right) \mathrm{C}_{if} \mathrm{d}E_f \ , \tag{58.179}$$

and macroscopic detailed balance $\hat{\alpha}\tilde{N}_{\mathrm{A}}\tilde{N}_{\mathrm{B}} = k\tilde{n}_{\mathrm{s}}$ is automatically satisfied; $\hat{\alpha}$ is the direct ($C \to S$) collisional contribution (small) plus the (much larger) net collisional cascade downward contribution from that fraction of bound levels that originated in the continuum C; k_d is the direct dissociation frequency (small) plus the net collisional cascade upward contribution from that fraction of bound levels that originated in block S.

58.10.2 Time-Independent Methods: Low Gas Density

QSS rate

Since recombination and dissociation (ionization) involve only that fraction of the bound state population that originated from the C and S blocks, respectively, recombination can be viewed as time independent with

$$N_{\mathrm{A}}\, N_{\mathrm{B}} = \tilde{N}_{\mathrm{A}}\tilde{N}_{\mathrm{B}}, \ \ n_{\mathrm{s}}(t) = 0 \ , \tag{58.180a}$$

$$\rho_i = n_i/\tilde{n}_i \equiv P_i^{\mathrm{D}} \tag{58.180b}$$

$$\hat{\alpha}\tilde{N}_{\mathrm{A}}\tilde{N}_{\mathrm{B}} = \int_{-E}^{\infty} \mathrm{d}E_i \int_{-D}^{-E} (\rho_i - \rho_f) \mathrm{C}_{if} \mathrm{d}E_f \ . \tag{58.180c}$$

QSS integral equation

$$\rho_i \int_{-D}^{\infty} \nu_{if} \mathrm{d}E_f = \int_{-S}^{\infty} \rho_f \nu_{if} \mathrm{d}E_f \tag{58.181}$$

is solved subject to the boundary condition

$$\rho_i = 1 (E_i \geq 0) \ , \quad \rho_i = 0 (-S \geq E_i \geq -D) \ . \tag{58.182}$$

Collisional energy-change moments

$$D^{(m)}(E_i) = \frac{1}{m!}\int_{-D}^{\infty}(E_f - E_i)^m \mathrm{C}_{if}\,\mathrm{d}E_f\ , \qquad (58.183)$$

$$D_i^{(m)} = \frac{1}{m!}\frac{\mathrm{d}}{\mathrm{d}t}\langle(\Delta E)^m\rangle\ . \qquad (58.184)$$

Averaged energy-change frequency
For an equilibrium distribution $\tilde{n}_i$ of E_i-pairs per unit interval $\mathrm{d}E_i$ per second,

$$D_i^{(1)} = \frac{\mathrm{d}}{\mathrm{d}t}\langle\Delta E\rangle\ .$$

Averaged energy-change per collision

$$\langle\Delta E\rangle = D_i^{(1)}/D_i^{(0)}\ .$$

Time-independent dissociation
The time-independent picture corresponds to

$$n_\mathrm{s}(t) = \tilde{n}_\mathrm{s},\quad \gamma_\mathrm{c}(t) = 0,\quad \rho_i = n_i/\tilde{n}_i \equiv P_i^\mathrm{S}\ , \qquad (58.185)$$

in analogy to the macroscopic reduction of Eqs. (58.50a,58.50b).

Variational Principle

The QSS condition Eq. (58.174) implies that the fraction P_i^D of bound levels i with precursor C are so distributed over i that Eq. (58.176) for $\hat{\alpha}$ is a minimum. Hence P_i^D or ρ_i are obtained either from the solution of Eq. (58.181) or from minimizing the variational functional

$$\hat{\alpha}\tilde{N}_\mathrm{A}\tilde{N}_\mathrm{B} = \int_{-D}^{\infty} n_i\mathrm{d}E_i\int_{-D}^{\infty}\left(\rho_i - \rho_f\right)\nu_{if}\mathrm{d}E_f \qquad (58.186a)$$

$$= \frac{1}{2}\int_{-D}^{\infty}\mathrm{d}E_i\int_{-D}^{\infty}\left(\rho_i - \rho_f\right)^2\mathrm{C}_{if}\mathrm{d}E_f\ , \qquad (58.186b)$$

with respect to variational parameters contained in a trial analytic expression for ρ_i. Minimization of the quadratic functional Eq. (58.186b) has an analogy with the principle of least dissipation in the theory of electrical networks.

Diffusion-in-Energy-Space Method

Integral Eq. (58.181) can be expanded in terms of energy-change moments, via a Fokker–Planck analysis to yield the differential equation

$$\frac{\partial}{\partial E_i}\left(D_i^{(2)}\frac{\partial\rho_i}{\partial E_i}\right) = 0\ , \qquad (58.187)$$

with the QSS analytical solution

$$\rho_i(E_i) = \left(\int_{E_i}^{0}\frac{\mathrm{d}E}{D^{(2)}(E)}\right)\left(\int_{-S}^{0}\frac{\mathrm{d}E}{D^{(2)}(E)}\right)^{-1} \qquad (58.188)$$

of *Pitaevskii* [33] for $(\mathrm{e}^- + \mathrm{A}^+ + \mathrm{M})$ recombination where collisional energy changes are small. This distribution does not satisfy the exact QSS condition Eq. (58.181). When inserted in the exact non-QSS rate Eq. (58.186b), highly accurate $\hat{\alpha}$ for heavy-particle recombination are obtained.

Bottleneck Method

The one-way equilibrium rate ($\mathrm{cm}^{-3}\,\mathrm{s}^{-1}$) across $-E$, i.e., Eq. (58.180c) with $\rho_i = 1$ and $\rho_f = 0$, is

$$\hat{\alpha}(-E)\tilde{N}_\mathrm{A}\tilde{N}_\mathrm{B} = \int_{-E}^{\infty}\mathrm{d}E_i\int_{-D}^{-E}\mathrm{C}_{if}\mathrm{d}E_f\ . \qquad (58.189)$$

This is an upper limit to Eq. (58.180c) and exhibits a minimum at $-E^*$, the bottleneck location. The least upper limit to $\hat{\alpha}$ is then $\hat{\alpha}(-E^*)$.

Trapping Radius Method

Assume that pairs with internal separation $R \le R_\mathrm{T}$ recombine with unit probability so that the one-way equilibrium rate across the dissociation limit at $E = 0$ for these pairs is

$$\hat{\alpha}(R_\mathrm{T})\tilde{N}_\mathrm{A}\tilde{N}_\mathrm{B} = \int_0^{R_\mathrm{T}}\mathrm{d}\boldsymbol{R}\int_{V(R)}^{0}\mathrm{C}_{if}(R)\mathrm{d}E_f\ , \qquad (58.190)$$

where $V(R) = -e^2/R$, and $\mathrm{C}_{if}(R) = \tilde{n}_i(R)\nu_{if}(R)$ is the rate per unit interval $(\mathrm{d}\boldsymbol{R}\mathrm{d}E_i)\mathrm{d}E_f$ for the $E_i \to E_f$ collisional transitions at fixed R in

$$\left(\mathrm{A}^+ - \mathrm{B}^-\right)_{E_i,R} + \mathrm{M} \to \left(\mathrm{A}^+ - \mathrm{B}^-\right)_{E_f,R} + \mathrm{M}\ . \qquad (58.191)$$

The concentration (cm^{-3}) of pairs with internal separation R and orbital energy E_i in the interval $\mathrm{d}\boldsymbol{R}\mathrm{d}E_i$ about $(\boldsymbol{R}, E_i)$ is $\tilde{n}_i(R)\mathrm{d}\boldsymbol{R}\mathrm{d}E_i$. Agreement with the exact treatment [54] is found by assigning $R_\mathrm{T} = (0.48 - 0.55)(e^2/k_\mathrm{B}T)$ for the recombination of equal mass ions in an equal mass gas for various ion–neutral interactions.

58.10.3 Recombination at Higher Gas Densities

As the density N of the gas M is raised, the recombination rate $\hat{\alpha}$ increases initially as N to such an extent that there are increasingly more pairs $n_i^-(R, E)$ in a state of contraction in

R than there are those $n_i^+(R,E)$ in a state of expansion; i.e., the ion-pair distribution densities $n_i^\pm(R,E)$ per unit interval $\mathrm{d}E\,\mathrm{d}R$ are not in equilibrium with respect to R in blocks $\mathcal{C}$ and $\mathcal{E}$. Those in the highly excited block $\mathcal{E}$, in addition, are not in equilibrium with respect to energy E. Basic sets of coupled master equations have been developed [54] for the microscopic nonequilibrium distributions $n^\pm\big(R,E,L^2\big)$ and $n^\pm(R,E)$ of expanding (+) and contracting (−) pairs with respect to A–B separation R, orbital energy E, and orbital angular momentum L^2. With $n\big(\boldsymbol{R},E_i,L_i^2\big)\equiv n_i(R)$ and using the notation defined at the beginning of Sect. 58.6, the distinct regimes for the master equations discussed in Sect. 58.10.4 are:

Low N equilibrium in R, but not in E, L^2
→ master equation for $n\big(E,L^2\big)$.
Pure Coulomb equilibrium in L^2
Attraction → master equation for $n(E)$.
High N nonequilibrium in R, E, L^2
→ master equation for $n_i^\pm(R)$.
Highest N equilibrium in $\big(E,L^2\big)$ but not in R
→ macroscopic transport equation
Eq. (58.68a) in $n(R)$.

Normalized Distributions

For a state $\rangle i \equiv \rangle E,L^2$,

$$\rho_i(R)=\frac{n_i(R)}{\tilde{n}_i(R)},\quad \rho_i^\pm(R)=\frac{n_i^\pm(R)}{\tilde{n}_i^\pm(R)}\,,$$
$$\rho_i(R)=\frac{1}{2}\big(\rho_i^+ + \rho_i^-\big)\,. \tag{58.192}$$

Orbital Energy and Angular Momentum

$$E_i=\frac{1}{2}\mathrm{M_{AB}}v^2+V(R)\,, \tag{58.193a}$$
$$E_i=\frac{1}{2}\mathrm{M_{AB}}v_\mathrm{R}^2+V_i(R)\,, \tag{58.193b}$$
$$V_i(R)=V(R)+\frac{L_i^2}{2\mathrm{M_{AB}}R^2}\,, \tag{58.193c}$$
$$L_i=|\boldsymbol{R}\times\mathrm{M_{AB}}\boldsymbol{v}|\,,$$
$$L_i^2=(2\mathrm{M_{AB}}E_i)b^2,\ E_i>0\,. \tag{58.193d}$$

Maximum Orbital Angular Momenta

(1) A specified separation R can be accessed by all orbits of energy E_i with L_i^2 between 0 and

$$L_{i\mathrm{m}}^2(E_i,R)=2\mathrm{M_{AB}}R^2[E_i-V(R)]\,. \tag{58.194a}$$

(2) Bounded orbits of energy $E_i<0$ can have L_i^2 between 0 and

$$L_{i\mathrm{c}}^2(E_i)=2\mathrm{M_{AB}}R_\mathrm{c}^2[E_i-V(R_\mathrm{c})]\,, \tag{58.194b}$$

where R_c is the radius of the circular orbit determined by $\partial V_i/\partial R=0$, i.e., by $E_i=V(R_\mathrm{c})+\frac{1}{2}R_\mathrm{c}(\partial V/\partial R)_{R_\mathrm{c}}$.

58.10.4 Master Equations

Master Equation for $n_i^\pm(R)\equiv n^\pm\big(R,E_i,L_i^2\big)$ [54]

$$\pm\frac{1}{R^2}\frac{\partial}{\partial R}\big[R^2 n_i^\pm(R)|v_\mathrm{R}|\big]_{E_i,L_i^2}$$
$$=-\int_{V(R)}^{\infty}\mathrm{d}E_f\int_0^{L_{f\mathrm{m}}^2}\mathrm{d}L_f^2\Big[n_i^\pm(R)v_{if}(R)-n_f^\pm(R)v_{fi}(R)\Big]\,. \tag{58.195}$$

The set of master equations [54] for n_i^+ is coupled to the n_i^- set by the boundary conditions $n_i^-\big(R_i^\mp\big)=n_i^+\big(R_i^\mp\big)$ at the pericenter R_i^- for all E_i and apocenter R_i^+ for $E_i<0$ of the E_i,L_i^2-orbit.

Master Equations for Normalized Distributions [54]

$$\pm|v_\mathrm{R}|\frac{\partial\rho_i^\pm}{\partial R}=-\int_{V(R)}^{\infty}\mathrm{d}E_f\int_0^{L_{f\mathrm{m}}^2}\mathrm{d}L_f^2\times\Big[\rho_i^\pm(R)-\rho_f^\pm(R)\Big]v_{if}(R)\,. \tag{58.196}$$

Corresponding master equations for the L^2 integrated distributions $n^\pm(R,E)$ and $\rho^\pm(R,E)$ have been derived [54].

Continuity Equations

$$J_i=\big[n_i^+(R)-n_i^-(R)\big]|v_\mathrm{R}|=\big(\rho_i^+-\rho_i^-\big)\tilde{j}_i^\pm\,, \tag{58.197}$$
$$\frac{1}{R^2}\frac{\partial}{\partial R}(R^2J_i)=-\int_{V(R)}^{\infty}\mathrm{d}E_f\int_0^{L_{f\mathrm{m}}^2}\mathrm{d}L_f^2\times\big[n_i(R)v_{if}(R)-n_f(R)v_{fi}(R)\big]\,, \tag{58.198}$$
$$\frac{1}{2}|v_\mathrm{R}|\frac{\partial\big[\rho_i^+(R)-\rho_i^-(R)\big]}{\partial R}=-\int_{V(R)}^{\infty}\mathrm{d}E_f\int_0^{L_{f\mathrm{m}}^2}\mathrm{d}L_f^2\big[\rho_i(R)-\rho_f(R)\big]v_{if}(R)\,. \tag{58.199}$$

58.10.5 Recombination Rate

Flux Representation

The $R_0\to\infty$ limit of

$$\hat{\alpha}\tilde{N}_\mathrm{A}\tilde{N}_\mathrm{B}=-4\pi R_0^2J(R_0) \tag{58.200}$$

has the microscopic generalization

$$\hat{\alpha}\tilde{N}_{\mathrm{A}}\tilde{N}_{\mathrm{B}} = \int_{V(R_0)}^{\infty} \mathrm{d}E_i \int_0^{L_{ic}^2} \mathrm{d}L_i^2 \left[4\pi R_0^2 \tilde{j}_i^{\pm}(R_0)\right] \times \left[\rho_i^-(R_0) - \rho_i^+(R_0)\right] , \tag{58.201}$$

where L_{ic}^2 is given by Eq. (58.194b) with $R_c = R_0$ for bound states and is infinite for dissociated states, and where

$$\rho_i^-(R_0) - \rho_i^+(R_0) = \oint_{R_i}^{R_0} \rho_i(R)\left[v_i^b(R) + v_i^c(R)\right]\mathrm{d}t , \tag{58.202}$$

with

$$\rho_i(R)v_i^b(R) = \int_{V(R)}^{V(R_0)} \mathrm{d}E_f \int_0^{L_{fm}^2} \mathrm{d}L_f^2 \left[\rho_i(R) - \rho_f(R)\right] \times v_{if}(R) ,$$
$$\rho_i(R)v_i^c(R) = \int_{V(R_0)}^{\infty} \mathrm{d}E_f \int_0^{L_{fm}^2} \mathrm{d}L_f^2 \left[\rho_i(R) - \rho_f(R)\right] \times v_{if}(R) . \tag{58.203a}$$

Collisional Representation

$$\hat{\alpha}\tilde{N}_{\mathrm{A}}\tilde{N}_{\mathrm{B}} = \int_{V(R_0)}^{\infty} \mathrm{d}E_i \int_0^{L_{ic}^2} \mathrm{d}L_i^2 \int_{R_i}^{R_0} \tilde{n}_i(R)\,\mathrm{d}\boldsymbol{R} \times \left[\rho_i(R)v_i^b(R)\right] , \tag{58.204}$$

which is the microscopic generalization of the macroscopic result $\hat{\alpha} = K\rho^* v_{\mathrm{s}} = \alpha_{RN}(R_0)\rho(R_0)$.

The flux for dissociated pairs $E_i > 0$ is

$$4\pi R^2 |v_{\mathrm{R}}| \tilde{n}_i^{\pm}(R)\,\mathrm{d}E\,\mathrm{d}L^2 = [\overline{v}\varepsilon \mathrm{e}^{-\varepsilon}\,\mathrm{d}\varepsilon][2\pi b\,\mathrm{d}b]\tilde{N}_{\mathrm{A}}\tilde{N}_{\mathrm{B}} , \tag{58.205}$$

so the rate Eq. (58.204) as $R_0 \to \infty$ is

$$\hat{\alpha} = \overline{v} \int_0^{\infty} \varepsilon \mathrm{e}^{-\varepsilon}\,\mathrm{d}\varepsilon \int_0^{b_0} 2\pi b\,\mathrm{d}b \oint_{R_i}^{R_0} \rho_i(R)v_i^b(R)\,\mathrm{d}t , \tag{58.206}$$

which is the microscopic generalization Eq. (58.57b) of the macroscopic result $\hat{\alpha} = k_{\mathrm{c}} P^{\mathrm{S}}$ of Eq. (58.56).

Reaction Rate $\alpha_{RN}(R_0)$

On solving Eq. (58.196) subject to $\rho(R_0) = 1$, according to Eq. (58.68b), $\hat{\alpha}$ determined by Eq. (58.201) is the rate $\hat{\alpha}_{RN}$ of recombination within the (A − B) sphere of radius R_0. The overall rate of recombination $\hat{\alpha}$ is then given by the full diffusional-drift reaction rate Eq. (58.71b) where the rate of transport to R_0 is determined uniquely by Eq. (58.72).

58.11 Radiative Recombination

In the radiative recombination (RR) process

$$\mathrm{e}^-(E,\ell') + \mathrm{A}^{Z+}(c) \to \mathrm{A}^{(Z-1)+}(c, n\ell) + h\nu , \tag{58.207}$$

the accelerating electron e^- with energy and angular momentum (E,ℓ') is captured, via coupling with the weak quantum electrodynamic interaction $(e/m_{\mathrm{e}}c)\boldsymbol{A}\cdot\boldsymbol{p}$ associated with the electromagnetic field of the moving ion, into an excited state $n\ell$ with binding energy $I_{n\ell}$ about the parent ion A^{Z+} (initially in an electronic state c). The simultaneously emitted photon carries away the excess energy $h\nu = E + I_{n\ell}$ and angular momentum difference between the initial and final electronic states. The cross section $\sigma_{\mathrm{R}}^{n\ell}(E)$ for RR is calculated (a) from the Einstein A coefficient for free–bound transitions or (b) from the cross section $\sigma_{\mathrm{I}}^{n\ell}(h\nu)$ for photoionization (PI) via the detailed balance (DB) relationship appropriate to Eq. (58.207).

The rates $\langle v_{\mathrm{e}}\sigma_{\mathrm{R}}\rangle$ and averaged cross sections $\langle\sigma_{\mathrm{R}}\rangle$ for a Maxwellian distribution of electron speeds v_{e} are then determined from either

$$\hat{\alpha}_{\mathrm{R}}^{n\ell}(T_{\mathrm{e}}) = \overline{v}_{\mathrm{e}} \int_0^{\infty} \varepsilon\sigma_{\mathrm{R}}^{n\ell}(\varepsilon)\exp(-\varepsilon)\mathrm{d}\varepsilon = \overline{v}_{\mathrm{e}}\left\langle\sigma_{\mathrm{R}}^{n\ell}(T_{\mathrm{e}})\right\rangle , \tag{58.208}$$

where $\varepsilon = E/k_{\mathrm{B}}T_{\mathrm{e}}$, or from the Milne DB relation Eq. (58.281) between the forward and reverse macroscopic rates of Eq. (58.207). Using the hydrogenic semiclassical σ_I^n of *Kramers* [34], together with an asymptotic expansion [55] for the g-factor of *Gaunt* [56], the quantal/semiclassical cross section ratio in Eq. (58.287), *Seaton* [57] calculated $\hat{\alpha}_{\mathrm{R}}^{n\ell}$.

The rate of electron energy loss in RR is

$$\left\langle\frac{\mathrm{d}E}{\mathrm{d}t}\right\rangle_{n\ell} = n_{\mathrm{e}}\overline{v}_{\mathrm{e}}(k_{\mathrm{B}}T_{\mathrm{e}}) \int_0^{\infty} \varepsilon^2\sigma_{\mathrm{R}}^{n\ell}(\varepsilon)\mathrm{e}^{-\varepsilon}\mathrm{d}\varepsilon , \tag{58.209}$$

and the radiated power produced in RR is

$$\left\langle\frac{\mathrm{d}(h\nu)}{\mathrm{d}t}\right\rangle_{n\ell} = n_{\mathrm{e}}\overline{v}_{\mathrm{e}} \int_0^{\infty} \varepsilon h\nu\sigma_{\mathrm{R}}^{n\ell}(\varepsilon)\mathrm{e}^{-\varepsilon}\mathrm{d}\varepsilon . \tag{58.210}$$

Standard conversions

$$E = p_e^2/2m_e = \hbar^2 k_e^2/2m_e = k_e^2 a_0^2 \left(e^2/2a_0\right) \tag{58.211a}$$

$$= \kappa^2 \left(Z^2 e^2/2a_0\right) = \varepsilon \left(Z^2 e^2/2a_0\right) , \tag{58.211b}$$

$$E_\nu = h\nu = \hbar\omega = \hbar k_\nu c = (I_n + E) \tag{58.211c}$$

$$\equiv \left(1 + n^2\varepsilon\right)\left(Z^2 e^2/2n^2 a_0\right) , \tag{58.211d}$$

$$h\nu/I_n = 1 + n^2\varepsilon, \quad k_e^2 a_0^2 = 2E/\left(e^2/a_0\right) , \tag{58.211e}$$

$$k_\nu a_0 = (h\nu)\alpha/\left(e^2/a_0\right) , \tag{58.211f}$$

$$k_\nu^2/k_e^2 = (h\nu)^2/\left(2Em_e c^2\right) \tag{58.211g}$$

$$= \alpha^2 (h\nu)^2/\left[2E\left(e^2/a_0\right)\right] , \tag{58.211h}$$

$$I_H = e^2/2a_0, \quad \alpha = e^2/\hbar c = 1/137.0359895 ,$$

$$\alpha^{-2} = m_e c^2/\left(e^2/a_0\right) , \quad I_n = \left(Z^2/n^2\right) I_H . \tag{58.211i}$$

The electron and photon wavenumbers are k_e and k_ν, respectively.

58.11.1 Detailed Balance and Recombination-Ionization Cross Sections

Cross sections $\sigma_R^{n\ell}(E)$ and $\sigma_I^{n\ell}(h\nu)$ for radiative recombination (RR) into and photoionization (PI) out of level $n\ell$ of atom A are interrelated by the detailed balance relation

$$g_e g_A^+ k_e^2 \sigma_R^{n\ell}(E) = g_\nu g_A \, k_\nu^2 \sigma_I^{n\ell}(h\nu) , \tag{58.212}$$

where $g_e = g_\nu = 2$. Electronic statistical weights of A and A^+ are g_A and g_A^+, respectively. Thus, using Eq. (58.211g) for k_ν^2/k_e^2,

$$\sigma_R^{n\ell}(E) = \left(\frac{g_A}{2g_A^+}\right)\left(\frac{(h\nu)^2}{Em_e c^2}\right)\sigma_I^{n\ell}(h\nu) . \tag{58.213}$$

The statistical factors are:

(a) For $\left(A^+ + e^-\right)$ state $c\left[S_c, L_c; \varepsilon, \ell', m'\right]$:

$$g_A^+ = (2S_c + 1)(2L_c + 1) .$$

(b) For $A(n\ell)$ state $b[S_c, L_c; n, \ell]SL$

$$g_A = (2S + 1)(2L + 1) .$$

(c) For $n\ell$ electron outside a closed shell

$$g_A^+ = 1, g_A = 2(2\ell + 1) .$$

Cross sections are averaged over initial and summed over final degenerate states. For case (c),

$$\sigma_I^n = \frac{1}{n^2}\sum_{\ell=0}^{n-1}(2\ell + 1)\sigma_I^{n\ell} ; \tag{58.214a}$$

$$\sigma_R^n = \sum_{\ell=0}^{n-1} 2(2\ell + 1)\sigma_R^{n\ell} . \tag{58.214b}$$

58.11.2 Kramers Cross Sections, Rates, Electron Energy-Loss Rates, and Radiated Power for Hydrogenic Systems

These are all calculated from application of the detailed balance Eq. (58.212) to the original $\sigma_I^n(h\nu)$ of *Kramers* [34].

Semiclassical (Kramers) Cross Sections

For hydrogenic systems,

$$I_n = \frac{Z^2 e^2}{2n^2 a_0}, \quad h\nu = I_n + E . \tag{58.215}$$

The results below are expressed in terms of the quantities

$$b_n = \frac{I_n}{k_B T_e} , \tag{58.216}$$

$$\sigma_{I0}^n = \frac{64\pi a_0^2 \alpha}{3\sqrt{3}}\left(\frac{n}{Z^2}\right)$$

$$= 7.907071 \times 10^{-18}\left(n/Z^2\right) \mathrm{cm}^2 , \tag{58.217}$$

$$\sigma_{R0}(E) = \left(\frac{8\pi a_0^2 \alpha^3}{3\sqrt{3}}\right)\frac{\left(Z^2 e^2/a_0\right)}{E} , \tag{58.218}$$

$$\hat{\alpha}_0(T_e) = \overline{v}_e\left(\frac{8\pi a_0^2 \alpha^3}{3\sqrt{3}}\right)\frac{\left(Z^2 e^2/a_0\right)}{k_B T_e} . \tag{58.219}$$

PI and RR cross sections for level *n*

In the Kramer (K) semiclassical approximation,

$$_K\sigma_I^n(h\nu) = \left(\frac{I_n}{h\nu}\right)^3 \sigma_{I0}^n = {}_K\sigma_I^{n\ell}(h\nu) , \tag{58.220}$$

$$_K\sigma_R^n(E) = \sigma_{R0}(E)\left(\frac{2}{n}\right)\left(\frac{I_n}{I_n + E}\right) \tag{58.221}$$

$$= 3.897 \times 10^{-20}$$

$$\times \left[n\varepsilon\left(13.606 + n^2\varepsilon^2\right)\right]^{-1} \mathrm{cm}^2 ,$$

where ε is in units of eV and is given by

$$\varepsilon = E/Z^2 \equiv \left(2.585 \times 10^{-2}/Z^2\right)\left(T_e/300\right) . \tag{58.222}$$

Equation (58.221) illustrates that RR into low n at low E is favored.

Cross section for RR into level $n\ell$

$$ {}_{\mathrm{K}}\sigma_{\mathrm{R}}^{n\ell} = \left[(2\ell+1)/n^2\right] {}_{\mathrm{K}}\sigma_{\mathrm{R}}^{n} \,. \tag{58.223} $$

Rate for RR into level n

$$ \hat{\alpha}_{\mathrm{R}}^{n}(T_{\mathrm{e}}) = \hat{\alpha}_0(T_{\mathrm{e}})(2/n) b_n \, \mathrm{e}^{b_n} E_1(b_n) \,, \tag{58.224a} $$

which for large b_n (i.e., $k_{\mathrm{B}}T_{\mathrm{e}} \ll I_n$) tends to

$$ \hat{\alpha}_{\mathrm{R}}^{n}(T_{\mathrm{e}} \to 0) = \hat{\alpha}_0(T_{\mathrm{e}})(2/n) \times \left(1 - b_n^{-1} + 2b_n^{-2} - 6b_n^{-3} + \cdots\right) . \tag{58.224b} $$

The Kramers cross section for photoionization at threshold is $\sigma_{\mathrm{I}0}^{n}$, and

$$ \sigma_{\mathrm{R}0}^{n} = 2\sigma_{\mathrm{R}0}/n; \quad \hat{\alpha}_0^{n} = 2\hat{\alpha}_0/n \tag{58.225} $$

provide the corresponding Kramers cross section and rate for recombination as $E \to 0$ and $T_{\mathrm{e}} \to 0$, respectively.

RR Cross sections and rates into all levels $n \geq n_f$

$$ \sigma_{\mathrm{R}}^{\mathrm{T}}(E) = \int_{n_f}^{\infty} \sigma_{\mathrm{R}}^{n}(E) \, \mathrm{d}n = \sigma_{\mathrm{R}0}(E) \ln(1 + I_f/E) \,, \tag{58.226a} $$

$$ \hat{\alpha}_{\mathrm{R}}^{\mathrm{T}}(T_{\mathrm{e}}) = \hat{\alpha}_0(T_{\mathrm{e}})\left[\gamma + \ln b_f + \mathrm{e}^{b_f} E_1(b_f)\right] . \tag{58.226b} $$

Useful integrals

$$ \int_0^{\infty} \mathrm{e}^{-x} \ln x \, \mathrm{d}x = \gamma \,, \tag{58.227a} $$

$$ \int_b^{\infty} x^{-1} \mathrm{e}^{-x} \mathrm{d}x = E_1(b) \,, \tag{58.227b} $$

$$ \int_0^{b} \mathrm{e}^{x} E_1(x) \, \mathrm{d}x = \gamma + \ln b + \mathrm{e}^{b} E_1(b) \,, \tag{58.227c} $$

$$ \int_0^{b} [1 - x \, \mathrm{e}^{x} E_1(x)] \mathrm{d}x = \gamma + \ln b + \mathrm{e}^{b}(1-b) E_1(b) \,, \tag{58.227d} $$

where $\gamma = 0.5772157$ is Euler's constant, and $E_1(b)$ is the first exponential integral such that

$$ b \, \mathrm{e}^{b} E_1(b) \overset{b \gg 1}{\longrightarrow} 1 - b^{-1} + 2b^{-2} - 6b^{-3} + 24b^{-4} + \cdots \,. $$

Electron Energy Loss Rate

Energy loss rate for RR into level n

$$ \left\langle \frac{\mathrm{d}E}{\mathrm{d}t} \right\rangle_n = n_{\mathrm{e}} \hat{\alpha}_{\mathrm{R}}^{n}(T_{\mathrm{e}}) k_{\mathrm{B}} T_{\mathrm{e}} \left(\frac{1 - b_n \, \mathrm{e}^{b_n} E_1(b_n)}{\mathrm{e}^{b_n} E_1(b_n)} \right) , \tag{58.228a} $$

which for large b_n (i.e. $(k_{\mathrm{B}}T_{\mathrm{e}}) \ll I_n$) tends to

$$ n_{\mathrm{e}} \hat{\alpha}_{\mathrm{R}}^{n}(T_{\mathrm{e}}) k_{\mathrm{B}} T_{\mathrm{e}} \left(1 - b_n^{-1} + 3b_n^{-2} - 13b_n^{-3} + \cdots\right) , \tag{58.228b} $$

with Eq. (58.224a) for $\hat{\alpha}_{\mathrm{R}}^{n}$.

Energy loss rate for RR into all levels $n \geq n_f$

$$ \left\langle \frac{\mathrm{d}E}{\mathrm{d}t} \right\rangle = n_{\mathrm{e}} k_{\mathrm{B}} T_{\mathrm{e}} \hat{\alpha}_0(T_{\mathrm{e}}) \left[\gamma + \ln b_f + \mathrm{e}^{b_f} E_1(b_f)(1 - b_f)\right] \tag{58.229a} $$

$$ = n_{\mathrm{e}} (k_{\mathrm{B}} T_{\mathrm{e}}) \left[\hat{\alpha}_{\mathrm{R}}^{\mathrm{T}}(T_{\mathrm{e}}) - \hat{\alpha}_0(T_{\mathrm{e}}) b_f \, \mathrm{e}^{b_f} E_1(b_f)\right] , \tag{58.229b} $$

with Eqs. (58.226b) and (58.219) for $\hat{\alpha}_{\mathrm{R}}^{\mathrm{T}}$ and $\hat{\alpha}_0$.

Radiated Power

Radiated power for RR into level n

$$ \left\langle \frac{\mathrm{d}(h\nu)}{\mathrm{d}t} \right\rangle_n = n_{\mathrm{e}} \hat{\alpha}_{\mathrm{R}}^{n}(T_{\mathrm{e}}) I_n \left[b_n \, \mathrm{e}^{b_n} E_1(b_n)\right]^{-1} , \tag{58.230a} $$

which for large b_n (i.e. $(k_{\mathrm{B}}T_{\mathrm{e}}) \ll I_n$) tends to

$$ n_{\mathrm{e}} \hat{\alpha}_{\mathrm{R}}^{n}(T_{\mathrm{e}}) I_n \left(1 + b_n^{-1} - b_n^{-2} + 3b_n^{-3} + \cdots\right) . \tag{58.230b} $$

Radiated power for RR into all levels $n \geq n_f$

$$ \left\langle \frac{\mathrm{d}(h\nu)}{\mathrm{d}t} \right\rangle = n_{\mathrm{e}} \hat{\alpha}_0(T_{\mathrm{e}}) I_f \,. \tag{58.231} $$

To allow n-summation, rather than integration as in Eq. (58.226a), $1/2\sigma_{\mathrm{R}}^{n_f}$, $1/2\hat{\alpha}_{\mathrm{R}}^{n_f}$, $1/2\langle \mathrm{d}E/\mathrm{d}t\rangle_{n_f}$, and $1/2\langle \mathrm{d}(h\nu)/\mathrm{d}t\rangle_{n_f}$, respectively, are added to each of the above expressions. The expressions valid for bare nuclei of charge Z are also fairly accurate for recombination to a core of charge Z_{c} and atomic number Z_{A}, provided that Z is identified as $1/2(Z_{\mathrm{A}} + Z_{\mathrm{c}})$.

Differential cross sections for Coulomb elastic scattering

$$ \sigma_{\mathrm{c}}(E, \theta) = \frac{b_0^2}{4 \sin^4 \frac{1}{2}\theta} \,, \quad b_0^2 = (Ze^2/2E)^2 \,. \tag{58.232} $$

The integral cross section for Coulomb scattering by $\theta \geq \pi/2$ at energy $E = (3/2)k_{\mathrm{B}}T$ is

$$ \sigma_{\mathrm{c}}(E) = \pi b_0^2 = \frac{1}{9}\pi R_{\mathrm{e}}^2, \quad R_{\mathrm{e}} = e^2/k_{\mathrm{B}}T \,. \tag{58.233} $$

Photon emission probability

$$P_\nu = \sigma_{\rm R}^n(E)/\sigma_{\rm c}(E)\ . \tag{58.234a}$$

This is small and increases with decreasing n as

$$P_\nu(E) = \left(\frac{8\alpha^3}{3\sqrt{3}}\right)\frac{8}{n}\frac{E}{(e^2/a_0)}\left(\frac{I_n}{h\nu}\right)\ . \tag{58.234b}$$

58.11.3 Basic Formulae for Quantal Cross Sections

Radiative Recombination and Photoionization Cross Sections

The cross section $\sigma_{\rm R}^{n\ell}$ for recombination follows from the continuum-bound transition probability P_{if} per unit time. It is also provided by the detailed balance relation Eq. (58.212) in terms of $\sigma_{\rm I}^{n\ell}$, which follows from P_{fi}. The number of radiative transitions per second is

$$\begin{aligned}&\left[g_{\rm e}g_{\rm A}^+\rho(E)\,{\rm d}E\,{\rm d}\hat{\boldsymbol{k}}_{\rm e}\right]P_{if}\left[\rho(E_\nu)\,{\rm d}E_\nu\,{\rm d}\hat{\boldsymbol{k}}_\nu\right]\\ &= g_{\rm e}g_{\rm A}^+ v_{\rm e}\frac{{\rm d}\boldsymbol{p}_{\rm e}}{(2\pi\hbar)^3}\sigma_{\rm R}(\boldsymbol{k}_{\rm e}) = g_\nu g_{\rm A}\,c\frac{{\rm d}\boldsymbol{k}_\nu}{(2\pi)^3}\sigma_{\rm I}(\boldsymbol{k}_\nu)\ ,\end{aligned} \tag{58.235}$$

where the electron current ($\mathrm{cm^{-2}\,s^{-1}}$) is

$$\frac{v_{\rm e}{\rm d}\boldsymbol{p}_{\rm e}}{(2\pi\hbar)^3} = \left(\frac{2mE}{h^3}\right){\rm d}E\,{\rm d}\hat{\boldsymbol{k}}_{\rm e}\ , \tag{58.236}$$

and the photon current ($\mathrm{cm^{-2}\,s^{-1}}$) is

$$c\frac{{\rm d}\boldsymbol{k}_\nu}{(2\pi)^3} = c\frac{(h\nu)^2}{(2\pi\hbar c)^3}\,{\rm d}E_\nu\,{\rm d}\hat{\boldsymbol{k}}_\nu\ . \tag{58.237}$$

Time-dependent quantum electrodynamical interaction

$$\begin{aligned}V(\boldsymbol{r},t) &= \frac{e}{mc}\boldsymbol{A}\cdot\boldsymbol{p} = {\rm i}e\left(\frac{2\pi h\nu}{\mathcal{V}}\right)^{1/2}(\hat{\boldsymbol{\epsilon}}\cdot\boldsymbol{r})\,{\rm e}^{-{\rm i}(\boldsymbol{k}_\nu\cdot\boldsymbol{r}-\omega t)}\\ &\equiv V(\boldsymbol{r})\,{\rm e}^{{\rm i}\omega t}\ .\end{aligned} \tag{58.238}$$

In the dipole approximation, ${\rm e}^{-{\rm i}\boldsymbol{k}_\nu\cdot\boldsymbol{r}} \approx 1$.

Continuum-bound state-to-state probability

$$\begin{aligned}P_{if} &= \frac{2\pi}{\hbar}\left|V_{fi}\right|^2\delta[E_\nu - (E+I_n)]\\ V_{fi} &= \langle\Psi_{n\ell m}(\boldsymbol{r})V(\boldsymbol{r})\rangle\Psi_i(\boldsymbol{r},\boldsymbol{k}_{\rm e})\ .\end{aligned} \tag{58.239}$$

Number of photon states in volume $\mathcal{V}$

$$\rho\left(E_\nu,\hat{k}_\nu\right){\rm d}E_\nu\,{\rm d}\hat{\boldsymbol{k}}_\nu = \mathcal{V}(h\nu)^2/(2\pi\hbar c)^3\,{\rm d}E_\nu\,{\rm d}\hat{\boldsymbol{k}}_\nu \tag{58.240a}$$

$$= \mathcal{V}\left[\omega^2/(2\pi c)^3\right]{\rm d}\omega\,{\rm d}\hat{\boldsymbol{k}}_\nu\ . \tag{58.240b}$$

Continuum-bound transition rate

On summing over the two directions ($g_\nu = 2$) of polarization, the rate for transitions into all final photon states is

$$\begin{aligned}{\rm A}_{n\ell m}\left(E,\hat{\boldsymbol{k}}_{\rm e}\right) &= \int P_{if}\rho(E_\nu)\,{\rm d}E_\nu{\rm d}\hat{\boldsymbol{k}}_\nu\\ &= \frac{4e^2}{3\hbar}\frac{(h\nu)^3}{(3\hbar c)^3}\left|\langle\Psi_{n\ell m}|\boldsymbol{r}|\Psi_i(\boldsymbol{k}_{\rm e})\rangle\right|^2\ .\end{aligned} \tag{58.241}$$

Transition frequency: alternative formula

$${\rm A}_{n\ell m}\left(E,\hat{\boldsymbol{k}}_{\rm e}\right) = (2\pi/\hbar)\left|D_{fi}\right|^2\ , \tag{58.242}$$

where the dipole atom–radiation interaction coupling is

$$D_{fi}(\boldsymbol{k}_{\rm e}) = \left(\frac{2\omega^3}{3\pi c^3}\right)^{1/2}\langle\Psi_{n\ell m}|e\,\boldsymbol{r}|\Psi_i(\boldsymbol{k}_{\rm e})\rangle\ . \tag{58.243}$$

RR cross section into level (n,ℓ,m)

$$\begin{aligned}\sigma_{\rm R}^{n\ell m}(E) &= \frac{1}{4\pi}\int\sigma_{\rm R}^{n\ell m}(\boldsymbol{k}_{\rm e}){\rm d}\hat{\boldsymbol{k}}_e\\ &= \frac{h^3\rho(E)}{8\pi m_{\rm e}E}\int{\rm A}_{n\ell m}\left(E,\hat{\boldsymbol{k}}_{\rm e}\right){\rm d}\hat{\boldsymbol{k}}_e\ .\end{aligned} \tag{58.244}$$

RR cross section into level (n,ℓ)

$$\begin{aligned}\sigma_{\rm R}^{n\ell}(E) &= \frac{8\pi^2}{3}\left(\frac{(\alpha h\nu)^3}{2(e^2/a_0)E}\right)\rho(E)R_{\rm I}^{n\ell}(E)\ ,\\ R_{\rm I}^{n\ell}(E) &= \int{\rm d}\hat{\boldsymbol{k}}_e\sum_m\left|\langle\Psi_{n\ell m}|\boldsymbol{r}|\Psi_i(\boldsymbol{k}_{\rm e})\rangle\right|^2\ .\end{aligned} \tag{58.245}$$

Transition T-matrix for RR

$$\sigma_{\rm R}^{n\ell}(E) = \frac{\pi a_0^2}{(ka_0)^2}|T_{\rm R}|^2\rho(E)\ , \tag{58.246}$$

$$|T_{\rm R}|^2 = 4\pi^2\int\sum_m\left|D_{fi}\right|^2{\rm d}\hat{\boldsymbol{k}}_{\rm e}\ . \tag{58.247}$$

Photoionization cross section

From the detailed balance in Eq. (58.235), $\sigma_{\rm I}^{n\ell}$ is

$$\sigma_{\rm I}^{n\ell}(h\nu) = \left(\frac{8\pi^2}{3}\right)\alpha h\nu\left(\frac{g_{\rm A}^+}{g_{\rm A}}\right)\rho(E)R_{\rm I}^{n\ell}(E)\ . \tag{58.248}$$

Continuum wave function expansion

$$\Psi_i(\boldsymbol{k}_{\rm e},\boldsymbol{r}) = \sum_{\ell'm'}{\rm i}^{\ell'}\,{\rm e}^{{\rm i}\eta_{\ell'}}R_{E\ell'}(r)Y_{\ell'm'}\left(\hat{\boldsymbol{k}}_{\rm e}\right)Y_{\ell'm'}(\hat{\boldsymbol{r}})\ . \tag{58.249}$$

Energy normalization

With $\rho(E) = 1$,

$$\int\Psi_i(\boldsymbol{k}_{\rm e};\boldsymbol{r})\Psi_i^*\left(\boldsymbol{k}'_{\rm e};\boldsymbol{r}\right){\rm d}\boldsymbol{r} = \delta\left(E-E'\right)\delta\left(\hat{\boldsymbol{k}}_{\rm e}-\hat{\boldsymbol{k}}'_{\rm e}\right)\ . \tag{58.250}$$

Plane wave expansion

$$e^{i\boldsymbol{k}\cdot\boldsymbol{r}} = 4\pi \sum_{\ell=0}^{\infty} i^{\ell} j_{\ell}(kr) Y^{*}_{\ell m}(\hat{\boldsymbol{k}}) Y_{\ell m}(\hat{\boldsymbol{r}}) \,, \tag{58.251}$$

$$j_{\ell}(kr) \approx \sin\left(kr - \frac{1}{2}\ell\pi\right) \Big/ (kr) \,. \tag{58.252}$$

For bound states,

$$\Psi_{n\ell m}(\boldsymbol{r}) = R_{n\ell}(r) Y_{\ell m}(\hat{\boldsymbol{r}}) \,. \tag{58.253}$$

RR and PI cross sections and radial integrals

$$\sigma_{\mathrm{R}}^{n\ell}(E) = \frac{8\pi^2}{3}\left(\frac{(\alpha h\nu)^3}{2(e^2/a_0)E}\right)\rho(E) R_{\mathrm{I}}(E; n\ell) \,. \tag{58.254}$$

For an electron outside a closed core,

$$g_{\mathrm{A}}^{+} = 1, \quad g_{\mathrm{A}} = 2(2\ell+1) \,,$$

$$\sigma_{\mathrm{I}}^{n\ell}(h\nu) = \frac{4\pi^2 \alpha h\nu \rho(E)}{3(2\ell+1)} R_{\mathrm{I}}(E; n\ell) \,, \tag{58.255a}$$

$$R_{n\ell}^{\varepsilon,\ell'} = \int_0^{\infty} (R_{\varepsilon\ell'}\, r\, R_{n\ell}) r^2 \,\mathrm{d}r \,, \tag{58.255b}$$

$$R_{\mathrm{I}}(E; n\ell) = \ell \left| R_{n\ell}^{\varepsilon,\ell-1} \right|^2 + (\ell+1) \left| R_{n\ell}^{\varepsilon,\ell+1} \right|^2 . \tag{58.255c}$$

For an electron outside an unfilled core (c) in the process $(\mathrm{A}^{+} + \mathrm{e}^{-}) \to \mathrm{A}(n\ell)$, the weights are

State i: $[S_{\mathrm{c}}, L_{\mathrm{c}}; \varepsilon]$, $g_{\mathrm{A}}^{+} = (2S_{\mathrm{c}}+1)(2L_{\mathrm{c}}+1)$.
State f: $[(S_{\mathrm{c}}, L_{\mathrm{c}}; n\ell)S, L]$, $g_{\mathrm{A}} = (2S+1)(2L+1)$.

$$R_{\mathrm{I}}(E; n\ell) = \frac{(2L+1)}{(2L_{\mathrm{c}}+1)} \times \sum_{\ell'=\ell\pm1} \sum_{L'} (2L'+1) \begin{Bmatrix} \ell & L & L_{\mathrm{c}} \\ L' & \ell' & 1 \end{Bmatrix}^2 \times \ell_{\max} \left| \int_0^{\infty} (R_{\varepsilon\ell'}\, r\, R_{n\ell}) r^2 \,\mathrm{d}r \right|^2 . \tag{58.256}$$

This reduces to Eq. (58.255c) when the radial functions $R_{i,f}$ do not depend on $(S_{\mathrm{c}}, L_{\mathrm{c}}, S, L)$.

Cross Section for Dielectronic Recombination

$$\sigma_{\mathrm{DLR}}^{n\ell}(E) = \frac{\pi a_0^2}{(ka_0)^2} |T_{\mathrm{DLR}}(E)|^2 \rho(E) \,,$$

$$|T_{\mathrm{DLR}}(E)|^2 = 4\pi^2 \int \mathrm{d}\hat{\boldsymbol{k}}_{\mathrm{e}} \times \sum_j \left| \frac{\langle \Psi_f D \rangle \Psi_j \langle \Psi_j V \rangle \Psi_i(\boldsymbol{k}_{\mathrm{e}})}{(E - \varepsilon_j + i\Gamma_j/2)} \right|^2 , \tag{58.257}$$

which is the generalization of the T-matrix Eq. (58.247) to include the effect of intermediate doubly excited autoionizing states $\langle \Psi_j$ in energy resonance to within width Γ_j of the initial continuum state Ψ_i. The electrostatic interaction $V = e^2 \sum_{i=1}^{N} (\boldsymbol{r}_i - \boldsymbol{r}_{N+1})^{-1}$ initially produces dielectronic capture by coupling the initial state i with the resonant states j, which become stabilized by coupling via the dipole radiation field interaction $\boldsymbol{D} = \left(2\omega^3/3\pi c^3\right)^{1/2} \sum_{i=1}^{N+1} (e\boldsymbol{r}_i)$ to the final stabilized state f. The above cross section for Eq. (58.3) is valid for isolated, nonoverlapping resonances.

Continuum Wave Normalization and Density of States

The basic formulae Eq. (58.245) for $\sigma_{\mathrm{R}}^{n\ell}$ depends on the density of states $\rho(E)$, which in turn varies according to the particular normalization constant N adopted for the continuum radial wave,

$$R_{E\ell}(r) \approx N \sin\left(kr - \frac{1}{2}\ell\pi + \eta_{\ell}\right) \Big/ r \,, \tag{58.258}$$

in Eq. (58.249) where the phase is

$$\eta_{\ell} = \arg \Gamma(\ell + 1 + i\beta) - \beta \ln 2kr + \delta_{\ell} \,. \tag{58.259}$$

The phase corresponding to the Hartree–Fock short-range interaction is δ_{ℓ}. The Coulomb phase shift for electron motion under $\left(-Ze^2/r\right)$ is $(\eta_{\ell} - \delta_{\ell})$ with $\beta = Z/(ka_0)$.

For a plane wave $\phi_{\boldsymbol{k}}(\boldsymbol{r}) = N' \exp(i\boldsymbol{k}\cdot\boldsymbol{r})$,

$$\left\langle \phi_{\boldsymbol{k}}(\boldsymbol{r}) | \phi_{\vec{k}'}(\boldsymbol{r}) \right\rangle \mathrm{d}\boldsymbol{k} = (2\pi)^3 |N'|^2 \rho(\boldsymbol{k})\, \mathrm{d}\boldsymbol{k}\, \delta(\boldsymbol{k} - \mathbf{k}') \equiv \left(\frac{h^3}{mp}\right) |N'|^2 \rho(E, \hat{\boldsymbol{k}})\, \mathrm{d}E\, \mathrm{d}\hat{\boldsymbol{k}}\, \delta(E - E') \delta(\hat{\boldsymbol{k}} - \hat{\boldsymbol{k}}') \,. \tag{58.260}$$

On integrating Eq. (58.260) over all E and $\hat{\boldsymbol{k}}$ for a single particle distributed over all $|E, \hat{\boldsymbol{k}}\rangle$ states, N' and ρ are then interrelated by

$$|N'|^2 \rho(E, \hat{\boldsymbol{k}}) = mp/h^3 \,. \tag{58.261}$$

The incident current is

$$j\, \mathrm{d}E\, \mathrm{d}\hat{\boldsymbol{k}}_{\mathrm{e}} = v |N'|^2 \rho(E, \hat{\boldsymbol{k}})\, \mathrm{d}E\, \mathrm{d}\hat{\boldsymbol{k}}_{\mathrm{e}} \tag{58.262a}$$

$$= (2mE/h^3)\mathrm{d}E\, \mathrm{d}\hat{\boldsymbol{k}}_{\mathrm{e}} = v\, \mathrm{d}\boldsymbol{p}_{\mathrm{e}}/h^3 \,. \tag{58.262b}$$

Radial wave connection

From Eqs. (58.249) and (58.251), $N = (4\pi N'/k)$, so that the connection between N of Eq. (58.258) and $\rho(E)$ is

$$|N|^2 \rho(E, \hat{\boldsymbol{k}}) = \frac{(2m/\hbar^2)}{\pi k} = \frac{(2/\pi)}{ka_0 e^2} \,. \tag{58.263}$$

RR Cross Sections for Common Normalization Factors of Continuum Radial Functions (Four Choices)

Choice a

$$N = 1; \quad \rho(E) = \frac{(2m/\hbar^2)}{\pi k} = \frac{(2/\pi)}{(ka_0)e^2} , \tag{58.264}$$

$$\sigma_{\mathrm{R}}^{n\ell}(E) = \frac{8\pi^2 a_0^2}{(ka_0)^3} \int \sum_m |D_{fi}|^2 \mathrm{d}\hat{\boldsymbol{k}}_{\mathrm{e}} , \tag{58.265}$$

where D_{fi} of Eq. (58.243) is dimensionless.

Choice b

$$N = k^{-1}; \quad \rho(E) = (2m/\hbar^2)(k/\pi) , \tag{58.266}$$

$$\sigma_{\mathrm{R}}^{n\ell}(E) = \frac{16\pi a_0^2}{3\sqrt{2}} \left(\frac{\alpha h\nu}{e^2/a_0}\right)^3 \sqrt{\frac{(e^2/a_0)}{E}} \left(\frac{R_{\mathrm{I}}}{a_0^5}\right), \tag{58.267}$$

where Eqs. (58.255b) and (58.255c) for R_{I} have dimension $[L^5]$.

Choice c

$$N = k^{-1/2}; \quad \rho(E) = \frac{(2m/\hbar^2)}{\pi} , \tag{58.268}$$

$$\sigma_{\mathrm{R}}^{n\ell}(E) = \frac{8\pi a_0^2}{3} \left(\frac{\alpha^3 (h\nu)^3}{(e^2/a_0)^2 E}\right) \left(\frac{R_{\mathrm{I}}}{a_0^4}\right) , \tag{58.269}$$

where R_{I} has dimensions of $[L^4]$.

Choice d

$$N = \left(2m/\hbar^2\pi^2 E\right)^{1/4}; \quad \rho(E) = 1 , \tag{58.270}$$

$$\sigma_{\mathrm{R}}^{n\ell}(E) = \frac{4(\pi a_0)^2}{3} \left(\frac{\alpha^3 (h\nu)^3}{(e^2/a_0)^2 E}\right) \left(\frac{R_{\mathrm{I}}}{e^2 a_0}\right) , \tag{58.271}$$

where R_{I} has dimensions of $[L^2 E^{-1}]$.

58.11.4 Bound–Free Oscillator Strengths

For a transition $n\ell \to E$ to $E + \mathrm{d}E$,

$$\frac{\mathrm{d}f_{n\ell}}{\mathrm{d}E} = \frac{2}{3} \frac{(h\nu)}{(e^2/a_0)} \frac{1}{(2\ell+1)} \sum_m \sum_{\ell' m'} \left| \boldsymbol{r}_{n\ell m}^{\varepsilon \ell' m'} \right|^2 , \tag{58.272}$$

$$R_{\mathrm{I}}(\varepsilon; n\ell) = \int \mathrm{d}\hat{\boldsymbol{k}}_e \sum_m |\langle \Psi_{n\ell m} | \boldsymbol{r} | \Psi_i(\boldsymbol{k}_{\mathrm{e}}) \rangle E|^2 = \sum_{m,\ell',m'} \left| \boldsymbol{r}_{n\ell m}^{\varepsilon \ell' m'} \right|^2 , \tag{58.273}$$

$$\sigma_{\mathrm{R}}^{n\ell}(E) = 2\pi^2 \alpha a_0^2 g_{\mathrm{A}} \left(\frac{k_v^2}{k_{\mathrm{e}}^2}\right) \left(\frac{e^2}{a_0}\right) \frac{\mathrm{d}f_{n\ell}}{\mathrm{d}E} , \tag{58.274a}$$

$$\sigma_{\mathrm{I}}^{n\ell}(h\nu) = 2\pi^2 \alpha a_0^2 g_{\mathrm{A}}^{+} \left(\frac{e^2}{a_0}\right) \frac{\mathrm{d}f_{n\ell}}{\mathrm{d}E} . \tag{58.274b}$$

Semiclassical Hydrogenic Systems

$$g_{\mathrm{A}} = g_{n\ell} = 2(2\ell+1) , \quad g_{\mathrm{A}}^{+} = 1 ,$$

$$\sigma_{\mathrm{R}}^{n}(E) = \sum_{\ell=0}^{n-1} \sigma_{\mathrm{R}}^{n\ell}(E) = 2\pi^2 \alpha a_0^2 \left(\frac{k_v^2}{k_{\mathrm{e}}^2}\right) \frac{\mathrm{d}F_n}{\mathrm{d}E} , \tag{58.275}$$

$$\frac{\mathrm{d}F_n}{\mathrm{d}E} = \sum_{\ell=0}^{n-1} g_{n\ell} \frac{\mathrm{d}f_{n\ell}}{\mathrm{d}E} = 2 \sum_{\ell,m} \frac{\mathrm{d}f_{n\ell m}}{\mathrm{d}E} . \tag{58.276}$$

Bound–bound absorption oscillator strength

For a transition $n \to n'$,

$$F_{nn'} = 2 \sum_{\ell m} \sum_{\ell' m'} f_{n\ell m}^{n'\ell' m'} \tag{58.277a}$$

$$= \frac{2^6}{3\sqrt{3}\pi} \left[\left(\frac{1}{n^2} - \frac{1}{n'^2} \right)^{-3} \right] \frac{1}{n^3} \frac{1}{n'^3} , \tag{58.277b}$$

$$\frac{\mathrm{d}F_n}{\mathrm{d}E} = \frac{2^5}{3\sqrt{3}\pi} n \frac{I_n^2}{(h\nu)^3} = 2n^2 \frac{\mathrm{d}f_{n\ell}}{\mathrm{d}E} , \tag{58.277c}$$

$$\sigma_{\mathrm{R}}^{n}(E) = \frac{2^5 \alpha^3}{3\sqrt{3}} \left(\frac{n I_n^2}{E(h\nu)} \right) \pi a_0^2 , \tag{58.277d}$$

$$\sigma_{\mathrm{I}}^{n\ell}(h\nu) = \frac{2^6 \alpha}{3\sqrt{3}} \frac{n}{Z^2} \left(\frac{I_n}{h\nu} \right)^3 \pi a_0^2 , \tag{58.277e}$$

$$= 7.907071 \left(\frac{n}{Z^2} \right) \left(\frac{I_n}{h\nu} \right)^3 \mathrm{Mb} . \tag{58.277f}$$

This semiclassical analysis yields exactly Kramers PI and associated RR cross sections in Sect. 58.8.2.

58.11.5 Radiative Recombination Rate

$$\hat{\alpha}_{\mathrm{R}}^{n\ell}(T_{\mathrm{e}}) = \overline{v}_{\mathrm{e}} \int_0^\infty \varepsilon \, \sigma_{\mathrm{R}}^{n\ell}(\varepsilon) \, \mathrm{e}^{-\varepsilon} \, \mathrm{d}\varepsilon \tag{58.278a}$$

$$\equiv \overline{v}_{\mathrm{e}} \langle \sigma_{\mathrm{R}}^{n\ell}(T_{\mathrm{e}}) \rangle , \tag{58.278b}$$

where ε is given in Eq. (58.57c), and $\langle \sigma_{\mathrm{R}}^{n\ell}(T_{\mathrm{e}}) \rangle$ is the Maxwellian-averaged cross section for radiative recombination.

In terms of the continuum-bound $\mathrm{A}_{n\ell}(E)$,

$$\hat{\alpha}_{\mathrm{R}}^{n\ell}(T_{\mathrm{e}}) = \frac{h^3}{(2\pi m_{\mathrm{e}} k_{\mathrm{B}} T)^{3/2}} \int_0^\infty \left(\frac{\mathrm{d}\mathrm{A}_{n\ell}}{\mathrm{d}\varepsilon} \right) \mathrm{e}^{-\varepsilon} \, \mathrm{d}\varepsilon , \tag{58.279}$$

$$\frac{\mathrm{d}\mathrm{A}_{n\ell}}{\mathrm{d}E} = \rho(E) \sum_m \int \mathrm{A}_{n\ell m}(E, \hat{\boldsymbol{k}}_{\mathrm{e}}) \, \mathrm{d}\hat{\boldsymbol{k}}_{\mathrm{e}} . \tag{58.280}$$

Milne Detailed Balance Relation

In terms of $\sigma_{\rm I}^{n\ell}(h\nu)$,

$$\hat{\alpha}_{\rm R}^{n\ell}(T_{\rm e}) = \overline{v}_{\rm e}\left(\frac{g_{\rm A}}{2g_{\rm A}^{+}}\right)\left(\frac{k_{\rm B}T_{\rm e}}{mc^2}\right)\left(\frac{I_n}{k_{\rm B}T_{\rm e}}\right)^2\left\langle\sigma_{\rm I}^{n\ell}(T_{\rm e})\right\rangle , \quad (58.281)$$

where, in reduced units $\omega = h\nu/I_n$, $T = k_{\rm B}T_{\rm e}/I_n = b_n^{-1}$, the averaged PI cross section corresponding to Eq. (58.213) is

$$\left\langle\sigma_{\rm I}^{n\ell}(T)\right\rangle = \frac{{\rm e}^{1/T}}{T}\int_1^\infty \omega^2\sigma_{\rm I}^{n\ell}(\omega)\,{\rm e}^{-\omega/T}\,{\rm d}\omega . \quad (58.282)$$

When $\sigma_{\rm I}^{n\ell}(\omega)$ is expressed in Mb ($10^{-18}\,{\rm cm}^2$),

$$\hat{\alpha}_{\rm R}^{n\ell}(T_{\rm e}) = 1.508\times10^{-13}\left(\frac{300}{T_{\rm e}}\right)^{1/2}\left(\frac{I_n}{I_{\rm H}}\right)^2\left(\frac{g_{\rm A}}{2g_{\rm A}^{+}}\right) \times\left\langle\sigma_{\rm I}^{n\ell}(T)\right\rangle{\rm cm}^3\,{\rm s}^{-1} . \quad (58.283)$$

When $\sigma_{\rm I}$ can be expressed in terms of the threshold cross section σ_0^n Eq. (58.217) as

$$\sigma_{\rm I}^{n\ell}(h\nu) = (I_n/h\nu)^p\sigma_0(n);(p=0,1,2,3) , \quad (58.284)$$

then $\left\langle\sigma_{\rm I}^{n\ell}(T)\right\rangle = S_p(T)\sigma_0(n)$, where

$$S_0(T) = 1+2T+2T^2 , \quad S_1(T) = 1+T , \quad (58.285a)$$
$$S_2(T) = 1 , \quad (58.285b)$$
$$S_3(T) = \left({\rm e}^{1/T}/T\right)E_1(1/T) \quad (58.285c)$$
$$\overset{T\ll1}{\approx} 1-T+2T^2-6T^3 . \quad (58.285d)$$

The case $p=3$ corresponds to Kramers PI cross section Eq. (58.220) so that

$${}_{\rm K}\hat{\alpha}_{\rm R}^{n\ell}(T_{\rm e}) = \frac{(2\ell+1)}{n^2}\frac{2}{n}\hat{\alpha}_0(T_{\rm e})S_3(T) \quad (58.286a)$$
$$\equiv {}_{\rm K}\hat{\alpha}_{\rm R}^{n\ell}(T_{\rm e}\to0)S_3(T) , \quad (58.286b)$$

such that ${}_{\rm K}\hat{\alpha}_{\rm R}^{n\ell} \approx Z^2/\left(n^3T_{\rm e}^{1/2}\right)$ as $T = (k_{\rm B}T_{\rm e}/I_n)\to0$.

58.11.6 Gaunt Factor, Cross Sections, and Rates for Hydrogenic Systems

The Gaunt factor $G_{n\ell}$ is the ratio of the quantal to Kramers (K) semiclassical PI cross section such that

$$\sigma_{\rm I}^{n\ell}(h\nu) = {}_{\rm K}\sigma_{\rm I}^{n}(h\nu)G_{n\ell}(\omega);\quad \omega = h\nu/I_n = 1+E/I_n . \quad (58.287)$$

(a) Radiative Recombination Cross Section

$$\sigma_{\rm R}^{n\ell}(E) = \left(\frac{g_{\rm A}}{g_{\rm A}^{+}}\right)\left(\frac{\alpha^2(h\nu)^2}{2E(e^2/a_0)}\right)G_{n\ell}(\omega)_{\rm K}\sigma_{\rm I}^{n}(h\nu) \quad (58.288a)$$
$$= G_{n\ell}(\omega)_{\rm K}\sigma_{\rm R}^{n\ell}(E) \quad (58.288b)$$
$$= \left[\frac{(2\ell+1)}{n^2}G_{n\ell}(\omega)\right]_{\rm K}\sigma_{\rm R}^{n}(E) , \quad (58.288c)$$
$$\sigma_{\rm R}^{n}(E) = G_n(\omega)_{\rm K}\sigma_{\rm R}^{n}(E) , \quad (58.288d)$$

where the quantum mechanical correction, or Gaunt factor, to the semiclassical cross sections

$$G_{n\ell}(\omega)\to\begin{cases}1, & \omega\to1\\ \omega^{-(\ell+1/2)}, & \omega\to\infty\end{cases} \quad (58.289)$$

favors low $n\ell$-states. The ℓ-averaged Gaunt factor is

$$G_n(\omega) = \left(1/n^2\right)\sum_{\ell=0}^{n-1}(2\ell+1)G_{n\ell}(\omega) . \quad (58.290)$$

Approximations for G_n: as ε increases from zero,

$$G_n(\varepsilon) = \left[1+\frac{4}{3}(a_n+b_n)+\frac{28}{18}a_n^2\right]^{-3/4} \quad (58.291a)$$
$$\simeq 1-(a_n+b_n)+\frac{7}{3}a_nb_n+\frac{7}{6}b_n^2 \quad (58.291b)$$

where $E = \varepsilon\left(Z^2e^2/2a_0\right)$, $\omega = 1+n^2\varepsilon$, and

$$a_n(\varepsilon) = 0.172825\left(1-n^2\varepsilon\right)c_n(\varepsilon) , \quad (58.292a)$$
$$b_n(\varepsilon) = 0.04959\left(1+\frac{4}{3}n^2\varepsilon+n^4\varepsilon^2\right)c_n^2(\varepsilon) , \quad (58.292b)$$
$$c_n(\varepsilon) = n^{-2/3}\left(1+n^2\varepsilon\right)^{-2/3} . \quad (58.292c)$$

Radiative Recombination Rate

$$\hat{\alpha}_{\rm R}^{n\ell}(T_{\rm e}) = {}_{\rm K}\hat{\alpha}_{\rm R}^{n\ell}(T_{\rm e}\to0)F_{n\ell}(T) , \quad (58.293)$$
$$\hat{\alpha}_{\rm R}^{n\ell}(T_{\rm e}\to0) = \frac{(2\ell+1)}{n^2}\left(\frac{2}{n}\right)\hat{\alpha}_0(T_{\rm e}) , \quad (58.294)$$

in accordance with Eq. (58.224b).

$$F_{n\ell}(T) = \frac{{\rm e}^{1/T}}{T}\int_1^\infty\frac{G_{n\ell}(\omega)}{\omega}{\rm e}^{-\omega/T}\,{\rm d}\omega . \quad (58.295)$$

The multiplicative factors F and G convert the semiclassical (Kramers) $T_{\rm e}\to0$ rate and cross section to their quantal values. Departures from the scaling rule $\left(Z^2/n^3T_{\rm e}^{1/2}\right)$ for RR rates is measured by $F_{n\ell}(T)$.

58.11.7 Exact Universal Rate Scaling Law and Results for Hydrogenic Systems

$$\hat{\alpha}_{\mathrm{R}}^{n\ell}(Z,T_{\mathrm{e}}) = Z\hat{\alpha}_{\mathrm{R}}^{n\ell}\left(1,T_{\mathrm{e}}/Z^2\right) \qquad (58.296)$$

as exhibited by Eq. (58.281) with Eqs. (58.277e) and (58.282).

Recombination rates are greatest into low n levels and the $\omega^{-\ell-1/2}$ variation of $G_{n\ell}$ preferentially populates states with low $\ell \approx 2$–5. Highly accurate analytical fits for $G_{n\ell}(\omega)$ have been obtained for $n \le 20$ so that Eq. (58.287) can be expressed in terms of known functions of fit parameters [58]. This procedure (which does not violate the S_2 sum rule) has been extended to nonhydrogenic systems of neon-like Fe XVII, where $\sigma_{\mathrm{I}}^{n\ell}(\omega)$ is a monotonically decreasing function of ω.

The variation of the ℓ-averaged values

$$n^{-2}\sum_{\ell=0}^{n-1}(2\ell+1)F_{n\ell}(T)$$

is close in both shape and magnitude to the corresponding semiclassical function $S_3(T)$, given by Eq. (58.295) with $G_{n\ell}(\omega) = 1$. Hence the ℓ-averaged recombination rate is

$$\hat{\alpha}_{\mathrm{R}}^{n}(Z,T) = (300/T)^{1/2}\left(Z^2/n\right)F_n(T)\ , \\ \times 1.1932\times10^{-12}\,\mathrm{cm}^3\,\mathrm{s}^{-1}\ ,$$

where F_n can be calculated directly from Eq. (58.295) or be approximated as $G_n(1)S(T)$. A computer program based on a three-term expansion of G_n is also available [59]. From a three-term expansion for G, the rate of radiative recombination into all levels of a hydrogenic system is

$$\hat{\alpha}(Z,T) = 5.2\times10^{-14}Z\lambda^{1/2} \\ \times\left(0.43+\frac{1}{2}\ln\lambda+0.47/\lambda^{1/2}\right), \qquad (58.297)$$

where $\lambda = 1.58\times10^5 Z^2/T$ and $[\hat{\alpha}] = \mathrm{cm}^3/\mathrm{s}$. Tables [60] exist for the effective rate

$$\hat{\alpha}_E^{n\ell}(T) = \sum_{n'=n}^{\infty}\sum_{\ell'=0}^{n'-1}\hat{\alpha}_{\mathrm{R}}^{n'\ell'}\mathrm{C}_{n'\ell',n\ell} \qquad (58.298)$$

of populating a given level $n\ell$ of H via radiative recombination into all levels $n' \ge n$ with subsequent radiative cascade $(i \to f)$ with probability $\mathrm{C}_{i,f}$ via all possible intermediate paths. Tables [60] also exist for the full rate

$$\hat{\alpha}_{\mathrm{F}}^{N}(T) = \sum_{n=N}^{\infty}\sum_{\ell=0}^{n-1}\hat{\alpha}_{\mathrm{R}}^{n\ell} \qquad (58.299)$$

of recombination, into all levels above $N = 1, 2, 3, 4$ of hydrogen. They are useful in deducing time scales of radiative recombination and rates for complex ions.

58.12 Useful Quantities

(a) Mean speed

$$\overline{v}_{\mathrm{e}} = \left(\frac{8k_{\mathrm{B}}T}{\pi m_{\mathrm{e}}}\right)^{1/2} = 1.076042\times10^7\left(\frac{T}{300}\right)^{1/2}\mathrm{cm/s} \\ = 6.69238\times10^7 T_{\mathrm{eV}}^{1/2}\,\mathrm{cm/s}\ , \\ \overline{v}_i = 2.51116\times10^5\left(\frac{T}{300}\right)^{1/2}\left(m_{\mathrm{p}}/m_i\right)^{1/2}\mathrm{cm/s}\ ,$$

where $(m_{\mathrm{p}}/m_{\mathrm{e}})^{1/2} = 42.850352$, and $T = 11604.45\,T_{eV}$ relates the temperature in K and in eV.

(b) Natural radius

$$|V(R_{\mathrm{e}})| = e^2/R_{\mathrm{e}} = k_{\mathrm{B}}T\ . \\ R_{\mathrm{e}} = \frac{e^2}{k_{\mathrm{B}}T} = 557\left(\frac{300}{T}\right)\text{Å} = \left(\frac{14.4}{T_{\mathrm{eV}}}\right)\text{Å}\ .$$

(c) Boltzmann average momentum

$$\langle p\rangle = \int_{-\infty}^{\infty}\mathrm{e}^{-p^2/2mk_{\mathrm{B}}T}\,\mathrm{d}p = (2\pi m_{\mathrm{e}}k_{\mathrm{B}}T)^{1/2}\ .$$

(d) De Broglie wavelength

$$\lambda_{\mathrm{dB}} = \frac{h}{\langle p\rangle} = \frac{h}{(2\pi m_{\mathrm{e}}k_{\mathrm{B}}T)^{1/2}} \\ = \frac{7.453818\times10^{-6}}{T_{\mathrm{e}}^{1/2}}\ \mathrm{cm} \\ = 43.035\left(\frac{300}{T_{\mathrm{e}}}\right)^{1/2}\text{Å} = \frac{6.9194}{T_{\mathrm{eV}}^{1/2}}\text{Å}\ .$$

References

1. Fendt, A.: Astrophys. J. Supp. Ser. **181**, 627 (2009)
2. Bernstein, J.: Kinetic theory in the expanding universe. Cambridge Univ. Press, Cambridge (1988). Chap. 8
3. Forrey, R.C.: Phys. Rev. A **88**, 052709 (2013)
4. Gordon, M.A., Sorochenko, R.L.: Radio Recombination Lines. 25 Years of Investigation. Kluwer, New York (1990)
5. Gordon, M.A., Sorochenko, R.L.: Radio Recombination Lines: Their Physics and Astronomical Applications. Kluwer, New York (2002)
6. Landsberg, P.T.: Recombination in Semiconductors. Cambridge Univ. Press, Cambridge (1991)
7. Lakhwani, G., Rao, A., Friend, R.H.: Ann. Rev. Phys. Chem. **65**, 557–581 (2014)
8. Del Zanna, G., Mason, H.E.: Liv. Rev. Solar Phys. **15**, 1–278 (2018)
9. Badnell, N.R., Del Zanna, G., Fernández-Menchero, L., Giunta, A.S., Liang, G.Y., Mason, H.E., Storey, P.J.: J. Phys. B. At. Mol. Opt. Phys. **49**, 094001 (2016)

10. Adamovich, et al.: J. Phys. D **50**, 323001 (2017)
11. Schinke, R., Grebenshchikov, S.Y., Ivanov, M.V., Fleurat-Lessard, P.: Ann. Rev. Phys. Chem. **57**, 625–661 (2006)
12. Burt, E.A., Ghrist, R.W., Myatt, C.J., Holland, M.J., Cornell, E.A., Wieman, C.E.: Phys. Rev. Lett. **79**, 337 (1997)
13. Nielsen, E., Macek, J.H.: Phys. Rev. Lett. **83**, 1566 (1999)
14. Ticknor, C., Rittenhouse, S.T.: Phys. Rev. Lett. **105**, 013201 (2010)
15. Truhlar, D.G., Wyatt, R.E.: Ann. Rev. Phys. Chem. **27**(1), 1–43 (1976)
16. Baer, M.: Theory of Chemical Reaction Dynamics vol. 1-4. CRC Press, Boca Raton, FL (1985)
17. Levine, R.D., Bernstein, R.B.: Molecular Reaction Dynamics and Chemical Reactivity. Oxford, New York (1987)
18. Butler, L.J.: Ann. Rev. Phys. Chem. **49**, 125–171 (1998)
19. Greene, S.M., Shan, X., Clary, D.C.: Adv. Chem. Phys. **163**, 117–149 (2018)
20. Greene, C.H., Giannakeas, P., Perez-Rios, J.: Rev. Mod. Phys. **89**, 035006 (2017)
21. Marcassa, L.G., Shaffer, J.P.: Adv. At. Mol. Opt. Phys. **63**, 47–133 (2014)
22. Scholes, G.D.: Ann. Rev. Phys. Chem. **54**, 57–87 (2003)
23. Flannery, M.R., Vrinceanu, D.: In: Oks, E., Pindzola, M.S. (eds.) Atomic Processes in Plasmas, pp. 317–333. American Institute of Physics, New York (1998)
24. Petrov, D.S., Werner, F.: Phys. Rev. A **92**, 022704 (2015)
25. Naidon, P., Endo, S.: Rep. Prog. Phys. **80**, 056001 (2017)
26. Braaten, E., Hammer, H.-W.: Phys. Rep. **428**, 259–390 (2006)
27. Mehta, N.P., Rittenhouse, S.T., D'Incao, J.P., von Stecher, J., Greene, C.H.: Phys. Rev. Lett. **103**, 153201 (2009)
28. Ferlaino, F., Knoop, S., Berninger, M., Harm, W., D'Incao, J.P., Nägerl, H.-C., Grimm, R.: Phys. Rev. Lett. **102**, 140401 (2009)
29. Ralchenko, Y.: Modern Methods in Collisional-Radiative Modeling of Plasmas. Springer, New York (2016)
30. Stevefelt, J., Boulmer, J., Delpech, J.-F.: Phys. Rev. A **12**, 1246 (1975)
31. Deloche, R., Monchicourt, P., Cheret, M., Lambert, F.: Phys. Rev. A **13**, 1140 (1976)
32. Mansbach, P., Keck, J.: Phys. Rev. **181**, 275 (1965)
33. Pitaevskii, L.P.: Sov. Phys. JETP **15**, 919 (1962)
34. Kramers, H.A.: Philos. Mag. **46**, 836 (1923)
35. Braaten, E., Kusunoki, M., Zhang, D.: Ann. Phys. **323**, 1770–1815 (2008)
36. Salomon, C., Shlyapnikov, G.V., Cugliandolo, L.F.: Many-Body Physics with Ultracold Gases. Oxford Univ. Press, Oxford (2013). Chap. 3
37. Bedaque, P.F., Braaten, E., Hammer, H.-W.: Phys. Rev. Lett. **85**, 908 (2000)
38. Braaten, E., Hammer, H.-W.: Phys. Rev. A **67**, 042706 (2003)
39. Efimov, V.: Phys. Lett. **33B**, 563 (1970)
40. Efimov, V.: Sov. J. Nucl. Phys. **12**, 589 (1971)
41. Braaten, E., Hammer, H.-W.: Ann. Phys. **322**, 120–163 (2007)
42. Avery, J.: Hyperspherical Harmonics: Applications in Quantum Theory. Kluwer, Norwell (1989)
43. Bhardwaj, S., Son, S.-K., Hong, K.-H., Lai, C.-J., Kärtner, F., Santra, R.: Phys. Rev. A **88**, 053405 (2013)
44. Bates, D.R.: Phys. Rev. **78**, 492 (1950)
45. Bardsley, J.N.: J. Phys. A Proc. Phys. Soc. **1**, 365 (1968)
46. Flannery, M.R.: In: Schultz, D.R., Strayer, M.R., Macek, J.H. (eds.) Atomic Collisions: A Symposium in Honor of Christopher Bottcher, pp. 53–75. American Institute of Physics, New York (1995)
47. Giusti, A.: J. Phys. B **13**, 3867 (1980)
48. van der Donk, P., Yousif, F.B., Mitchell, J.B.A., Hickman, A.P.: Phys. Rev. Lett. **68**, 2252 (1992)
49. Guberman, S.L.: Phys. Rev. A **49**, R4277 (1994)
50. Flannery, M.R.: Int. J. Mass. Spectrom. Ion. Process. **149/150**, 597 (1995)
51. Tashiro, M., Kato, S.: In: Guberman, S.L. (ed.) Dissociative Recombination of Molecular Ions with Electrons, pp. 243–248. Kluwer, Norwell (2003)
52. Florescu-Mitchell, A.I., Mitchell, J.B.A.: Phys. Rep. **430**, 277–374 (2006)
53. Johnsen, R., Guberman, S.L.: Adv. At. Mol. Opt. Phys. **59**, 76–128 (2010)
54. Flannery, M.R.: J. Chem. Phys. **95**, 8205 (1991)
55. Burgess, A.: Mon. Not. R. Astron. Soc. **118**, 477 (1958)
56. Gaunt, J.A.: Philos. Trans. R. Soc. A **229**, 163 (1930)
57. Seaton, M.J.: Mon. Not. R. Astron. Soc. **119**, 81 (1959)
58. Rozsnyai, B.F., Jacobs, V.L.: Astrophys. J. **327**, 485 (1988)
59. Flower, D.R., Seaton, M.J.: Comp. Phys. Commun. **1**, 31 (1969)
60. Martin, P.G.: Astrophys. J. Supp. Ser. **66**, 125 (1988)
61. Fontes, C.J., Zhang, H.L., Abdallah Jr, J., Clark, R.E.H., Kilcrease, D.P., Colgan, J., Cunningham, R.T., Hakel, P., Magee, N.H., Sherrill, M.E.: J. Phys. B. At. Mol. Opt. Phys. **48**, 144014 (2015)

Edmund J. Mansky II Edmund J. Mansky II received his PhD from Georgia Institute of Technology in 1985. His theoretical work involves statistical mechanics of dense gases. In addition, his interests are three-body recombination processes and collisions involving Rydberg states of atoms and molecules at thermal and ultracold temperatures. His day job is programming heliophysics data for the scientific community.